Statistical Analysis of Pavement Profiler Data to Evaluate the Bump at the End of the Bridge

PUBLICATION NO. FHWA-HRT-21-037

MAY 2021

U.S. Department of Transportation
Federal Highway Administration

Research, Development, and Technology
Turner-Fairbank Highway Research Center
6300 Georgetown Pike
McLean, VA 22101-2296

FOREWORD

The bump at the end of the bridge (BEB) is one of the most prevalent factors impacting ride quality at a bridge's approach and departure and can be a safety hazard to motorists. Its causes, along with mitigation strategies, have been well researched, yet the BEB remains ubiquitous, leading to chronic maintenance activities. This report details the data collected from inertial pavement profilers used to quantify the BEB at numerous bridge approaches across the country. Many of the bridge approaches measured included Geosynthetic Reinforced Soil–Integrated Bridge Systems which were compared with bridge approach profiles for conventional abutment types. This report also presents statistical analyses of the profile data to evaluate the effects of different site and bridge structure characteristics on BEB magnitude and ride quality. This report may be useful for geotechnical, bridge, and pavement engineers, consultants, and contractors.

Cheryl A. Richter, P.E., Ph.D.
Director, Office of Infrastructure
Research and Development

TECHNICAL REPORT DOCUMENTATION PAGE

1. Report No. FHWA-HRT-21-037	2. Government Accession No.	3. Recipient's Catalog No.
4. Title and Subtitle Statistical Analysis of Pavement Profiler Data to Evaluate the Bump at the End of the Bridge		5. Report Date May 2021 6. Performing Organization Code 1YX01
7. Author(s) Debakanta Mishra (ORCID: 0000-0003-2354-1312), Jenn McAtee (ORCID: 0000-0003-1547-7592), Md Shahjalal Chowdhury (ORCID: 0000-0003-2134-880X), Bhaskar Chittoori (ORCID: 0000-0001-8583-1003), Erol Tutumluer (ORCID: 0000-0003-3945-167X), and Jennifer Nicks, Ph.D., P.E. (HRDI-40; ORCID: 0000-0001-7230-3578)		8. Performing Organization Report No.
9. Performing Organization Name and Address Engineering & Software Consultants, Inc. 14123 Robert Paris Court Chantilly, VA 20151 Boise State University 1910 University Drive Boise, ID 83725		10. Work Unit No. 11. Contract or Grant No. DTFH6117D00011L/693JJ318F000070
12. Sponsoring Agency Name and Address Office of Infrastructure Research and Development Federal Highway Administration 6300 Georgetown Pike McLean, VA 22101		13. Type of Report and Period Covered Technical Report; March 2018–June 2020 14. Sponsoring Agency Code HRDI-40
15. Supplementary Notes The Task Order Contracting Officer's Representative was Jennifer Nicks, Ph.D., P.E. (HRDI-40; ORCID: 0000-0001-7230-3578).		

16. Abstract

The roughness experienced at bridge approaches and departures, generally termed the bump at the end of the bridge (BEB), has been identified as one of the most prominent issues in the transportation industry. The BEB is usually detected qualitatively based on road user feedback, with maintenance strategies subsequently implemented to improve ride quality. The BEB and road roughness can cause many issues beyond user discomfort, including driving safety concerns, vehicle damage, increased maintenance requirements for both automobiles and bridge infrastructure, and decreased bridge service life. The BEB is a complex issue caused by multiple interactive factors. Several research efforts have focused on identifying factors contributing to the BEB problem and identifying suitable remedial measures; however, quantitative approaches should be employed to establish standardized "ride quality indices" that can be used among engineers to evaluate the condition of a particular bridge approach and subsequently evaluate the need for maintenance and rehabilitation efforts. Researchers explored potential methods, such as the International Roughness Index and rolling straightedge measurements, to quantify the roughness at bridge approaches and analyzed the advantages and disadvantages of each. The surface profiles for a sample of 66 bridges across the United States were evaluated using multiple segment lengths and filters in ProVAL (The Transtec Group 2015) to statistically analyze the effects of different site and bridge structure characteristics on the magnitude and roughness of the BEB. A segment length of 0.31 m (1 ft) was determined the most appropriate for bridge approach analyses. This report presents findings from this study and makes inferences regarding what factors may have the most significant effect on the BEB problem.

17. Key Words	18. Distribution Statement
Bump at the end of the bridge, BEB, inertial profiler, International Roughness Index, IRI, rolling straightedge, RSE, bridge approach roughness	No restrictions. This document is available to the public through the National Technical Information Service, Springfield, VA 22161. http://www.ntis.gov

19. Security Classif. (of this report)	20. Security Classif. (of this page)	21. No. of Pages	22. Price
Unclassified	Unclassified	92	N/A

SI* (MODERN METRIC) CONVERSION FACTORS

APPROXIMATE CONVERSIONS TO SI UNITS

Symbol	When You Know	Multiply By	To Find	Symbol
		LENGTH		
in	inches	25.4	millimeters	mm
ft	feet	0.305	meters	m
yd	yards	0.914	meters	m
mi	miles	1.61	kilometers	km
		AREA		
in^2	square inches	645.2	square millimeters	mm^2
ft^2	square feet	0.093	square meters	m^2
yd^2	square yard	0.836	square meters	m^2
ac	acres	0.405	hectares	ha
mi^2	square miles	2.59	square kilometers	km^2
		VOLUME		
fl oz	fluid ounces	29.57	milliliters	mL
gal	gallons	3.785	liters	L
ft^3	cubic feet	0.028	cubic meters	m^3
yd^3	cubic yards	0.765	cubic meters	m^3
		NOTE: volumes greater than 1,000 L shall be shown in m^3		
		MASS		
oz	ounces	28.35	grams	g
lb	pounds	0.454	kilograms	kg
T	short tons (2,000 lb)	0.907	megagrams (or "metric ton")	Mg (or "t")
		TEMPERATURE (exact degrees)		
°F	Fahrenheit	5 (F-32)/9 or (F-32)/1.8	Celsius	°C
		ILLUMINATION		
fc	foot-candles	10.76	lux	lx
fl	foot-Lamberts	3.426	$candela/m^2$	cd/m^2
		FORCE and PRESSURE or STRESS		
lbf	poundforce	4.45	newtons	N
lbf/in^2	poundforce per square inch	6.89	kilopascals	kPa

APPROXIMATE CONVERSIONS FROM SI UNITS

Symbol	When You Know	Multiply By	To Find	Symbol
		LENGTH		
mm	millimeters	0.039	inches	in
m	meters	3.28	feet	ft
m	meters	1.09	yards	yd
km	kilometers	0.621	miles	mi
		AREA		
mm^2	square millimeters	0.0016	square inches	in^2
m^2	square meters	10.764	square feet	ft^2
m^2	square meters	1.195	square yards	yd^2
ha	hectares	2.47	acres	ac
km^2	square kilometers	0.386	square miles	mi^2
		VOLUME		
mL	milliliters	0.034	fluid ounces	fl oz
L	liters	0.264	gallons	gal
m^3	cubic meters	35.314	cubic feet	ft^3
m^3	cubic meters	1.307	cubic yards	yd^3
		MASS		
g	grams	0.035	ounces	oz
kg	kilograms	2.202	pounds	lb
Mg (or "t")	megagrams (or "metric ton")	1.103	short tons (2,000 lb)	T
		TEMPERATURE (exact degrees)		
°C	Celsius	1.8C+32	Fahrenheit	°F
		ILLUMINATION		
lx	lux	0.0929	foot-candles	fc
cd/m^2	candela/m2	0.2919	foot-Lamberts	fl
		FORCE and PRESSURE or STRESS		
N	newtons	2.225	poundforce	lbf
kPa	kilopascals	0.145	poundforce per square inch	lbf/in^2

*SI is the symbol for International System of Units. Appropriate rounding should be made to comply with Section 4 of ASTM E380. (Revised March 2003)

TABLE OF CONTENTS

LIST OF FIGURES

LIST OF TABLES

LIST OF ABBREVIATIONS

ADT	average daily traffic
ANOVA	analysis of variance
BEB	bump at the end of the bridge
DOT	department of transportation
FHWA	Federal Highway Administration
GRS-IBS	Geosynthetic Reinforced Soil–Integrated Bridge System
ID	identification
IRI	International Roughness Index
LTBP	Long-Term Bridge Performance
LTPP	Long-Term Pavement Performance
N/A	not applicable
Perp_Conv	Perpendicular-Conventional
Perp_GRS	Perpendicular GRS-IBS
ProVAL	Profile Viewing and Analysis Software
RSE	rolling straightedge
Skew_Conv	Skewed-Conventional
Skew_GRS	Skewed GRS-IBS

CHAPTER 1. INTRODUCTION AND BACKGROUND

One of the most chronic issues with roadway bridges is the bump at the end of the bridge (BEB) (Schaefer et al. 2013; Olmedo et al. 2015). The BEB occurs at the point of transition onto and off the bridge deck and can cause many issues, including user discomfort, vehicle damage, user safety concerns, and increased maintenance, among others (Henderson et al. 2016). Some common factors that cause the BEB are correlated to structural and geotechnical aspects of the bridge design; however, quantification of the pavement/deck roughness and the magnitude of the BEB is not common practice.

Several techniques and types of equipment can be used to measure a surface profile, including rod and level, walking profilers, rolling straightedge (RSE), profilograph, and inertial profilers (Sayers and Karamihas 1998; Zang et al. 2018; Mishra et al. 2020). Many transportation agencies across the country rely on inertial profilers for collecting profile data for pavements (Múčka 2017). This profile measurement process is preferred for its ability to collect information without impacting traffic (Henderson et al. 2016). As such, data collected from inertial profilers at bridge approaches were used for this study to remain consistent with current practice.

Using the data collected by the profilers, analyses can be performed by applying different wavelengths and filters to the raw data. The most common measurement rating for pavements is the International Roughness Index (IRI), which is currently used in countries around the world (Múčka 2017). To assess pavement performance, per a pavement rating system developed by the Federal Highway Administration (FHWA) to categorize the condition of interstate highways, an IRI value of less than 0.95 m/km (5.02 ft/mi) is considered a representation of "very good" conditions, whereas IRI values greater than 3.47 m/km (18.32 ft/mi) are representative of "very poor" conditions (Olmedo et al. 2015). An additional measurement rating is the RSE (McGhee 2002). Fortunately, the data collected by inertial profilers can be used in both measurement processes, making the data universally applicable.

The use of these measurement techniques is necessary to develop a quantitative method for establishing standardized quality indices. Based on information collected, methods of quantifying bridge approach roughness and BEB occurrences have been explored and are presented in this report.

OBJECTIVE AND SCOPE

The primary objective of this study was to analyze inertial profiler data collected at several different bridge approaches across the United States and evaluate trends related to factors that may significantly govern the phenomenon of the BEB. Initial analyses of the provided profiler data were performed using the commonly available software program Profile Viewing and Analysis (ProVAL) (The Transtec Group 2015). The collected data were also analyzed to assess the effectiveness of Geosynthetic Reinforced Soil–Integrated Bridge Systems (GRS-IBSs) as a potential design alternative to reduce bridge approach roughness.

The first sections of this report present general information regarding the processes used to make the IRI and RSE analyses applicable to the provided bridge and bridge-approach data. Details

about the data collected are also presented. After the descriptions of these generally applied methods and data, results obtained for specific bridges and categories are discussed in detail.

INTRODUCTION TO COMMONLY USED SURFACE PROFILE ROUGHNESS INDICES

The basic concepts of profile roughness measurement methods and commonly used indices are presented here to provide sufficient background information for the reader to understand the significance of the results obtained during the bridge analyses. There are various methods for measurement and rating of pavement profiles; the IRI is the most common rating method. However, according to Mishra et al. (2020, p. 12), "…factors of specific bridge lengths make [IRI measurements] unreliable as the only form of measurement." For this reason, the results of both the IRI and RSE rating methods were considered for the entirety of this project. The following sections describe the background behind these indices as well as the processes used for data analysis under the scope of this research study.

International Roughness Index

The IRI is a mathematical measurement model used as "a theoretical representation of the response-type systems in use at the time the IRI was developed" (Sayers and Karamihas 1998, p. 48). The development of this metric was a necessary process because different countries and State departments of transportation (DOTs) had different methods to determine road roughness at the time the IRI was developed. IRI models can be used to compare the results of different methods, providing an applicable standard for future data comparison across different agencies.

Application of IRI to Bridge Approaches

This study used calculated IRI values as the primary method to quantify the localized BEB roughness; RSE values were also evaluated and are discussed later in the Rolling Straightedge section of this report. An important component of the IRI measurement procedure is selecting an appropriate segment length to filter the profile data. Inertial profilers usually collect data at intervals of 25.4 mm (1 inch) or less (The Transtec Group 2015). When applying the IRI model to a particular profile in ProVAL, a segment length is necessary to reduce the number of intervals evaluated because they may not even be discernable by road users and are simply textural deviations. According to Múčka (2017), the most common segment length used to measure the localized road roughness of pavements is 7.62 m (25 ft).

By including a segment length in the ProVAL ride-quality analysis, the incremental data are converted to an overall IRI, continuous IRI, or fixed-interval IRI output. The overall IRI output produces a single roughness value for each path, the continuous IRI output produces multiple average values along each path, and the fixed-interval IRI output produces a value for each segment length along the path, appearing much like a bar graph (The Transtec Group 2015). For this study, the continuous IRI analysis type was selected, essentially converting the individual data points in a pavement profile into a moving average that reduces the pavement profile data and uses one representative IRI value per segment length (Henderson et al. 2016). Using continuous IRI output maintains the smooth-curve appearance of the collected data while eliminating excessive data to emphasize the IRI values that potentially indicate roughness or

BEB issues. The significance and basis of the segment lengths is further explained in the following section.

Significance of Segment Lengths

Although some recommendations are available concerning what segment lengths to use during the reduction of pavement profile data, no standards were found specifically to quantify the surface roughness at bridge approaches (Sayers and Karamihas 1998). Therefore, this research effort started by using a segment length of 7.62 m (25 ft) to reduce the bridge approach profile data to maintain consistency with the standard practice used by transportation agencies. With the understanding that the IRI measurement is a common tool used around the world for pavement surface roughness measurement, it was reasonable to start by using the same segment length as that used by most transportation agencies during roughness quantification of their respective pavement networks.

It is important to note that because of the "local" nature of the BEB problem (i.e., the roughness occurs at the interface between the roadway and the bridge structure), further analysis of the effects of segment length was performed before finalizing a particular technique for reducing the data for all 66 bridges. Accordingly, two additional segment lengths, 0.31 m (1 ft) and 3.05 m (10 ft), were used to reduce the data and study the effect of different segment lengths on the roughness quantification. Furthermore, each bridge location was divided into three sections—approach, bridge, and departure—to distinguish between the surface profile roughness when entering and exiting a bridge. The process for determining these sections is discussed in the Defining Bridge Approach and Departure Sections section at the end of this chapter. Along with the three sections of each bridge, there are three profiles indicated within each plot and dataset. These three profiles, labeled left, center, and right, are indicators of the location of the wheel profile within the lane. Although the profiles within a lane show some consistencies for long stretches of road, more distinct differences between the profiles can be seen as the length becomes shorter or the bridge is skewed.

As expected, the IRI values calculated from each profile data varied based on the segment length used in the analyses. For each bridge location, IRI traces could be established along the length of the bridge based on the different segment lengths. For example, figure 1 through figure 3 represent the IRI traces calculated for a bridge with a Skewed-Conventional (Skew_Conv) abutment as an example to demonstrate the impact of segment length on IRI values.

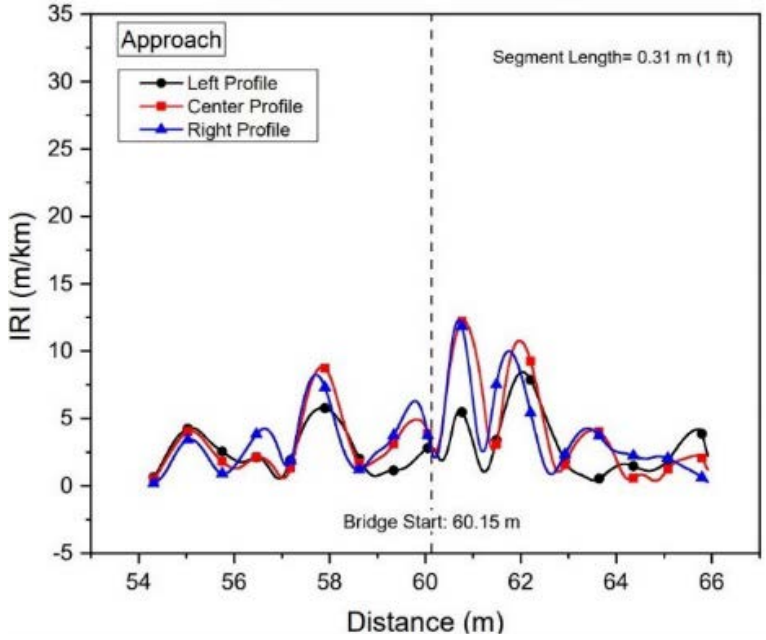

Source: FHWA.
1 m = 3.28 ft; 1 m/km = 5.28 ft/mi.

A. Approach section.

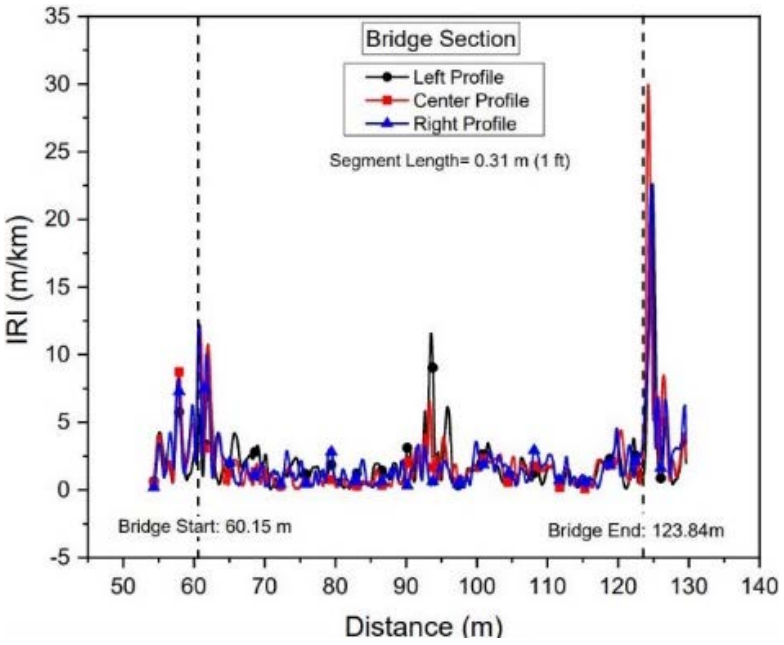

Source: FHWA.
1 m = 3.28 ft; 1 m/km = 5.28 ft/mi.

B. Bridge section.

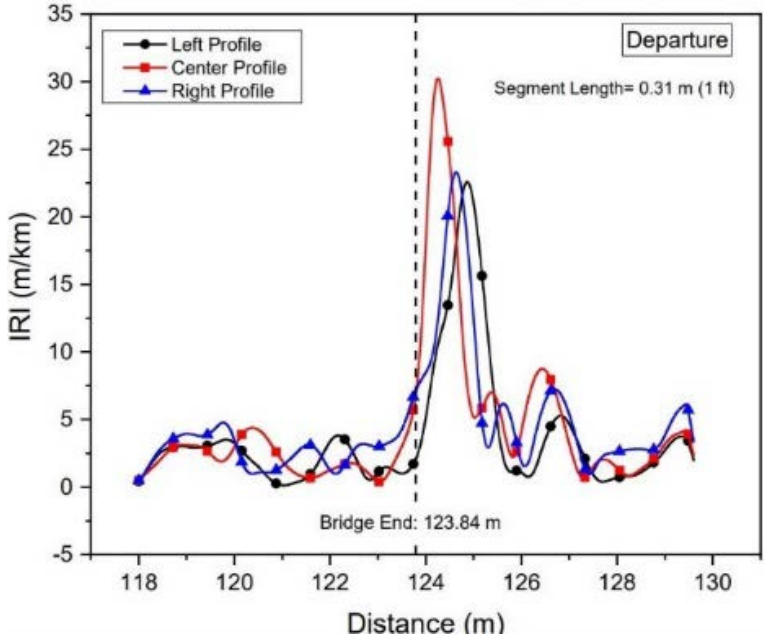

Source: FHWA.
1 m = 3.28 ft; 1 m/km = 5.28 ft/mi.

C. Departure section.

Figure 1. Graphs. IRI analysis with 0.31-m (1-ft) segment length for a Skew_Conv abutment.

Figure 1-A through figure 1-C represent the IRI data for the approach, bridge, and departure sections of the bridge, respectively, when segment lengths of 0.31 m (1 ft) were used. Similarly, figure 2-A through figure 2-C show the section data when segment lengths of 3.5 m (10 ft) were used, and figure 3-A through and figure 3-C show the section data when segment lengths of 7.62 m (25 ft) were used.

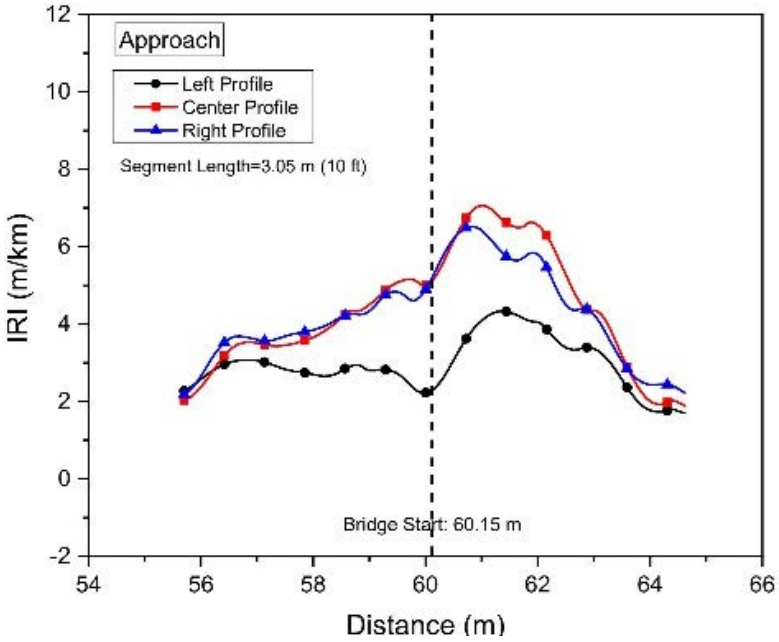

Source: FHWA.
1 m = 3.28 ft; 1 m/km = 5.28 ft/mi.

A. Approach section.

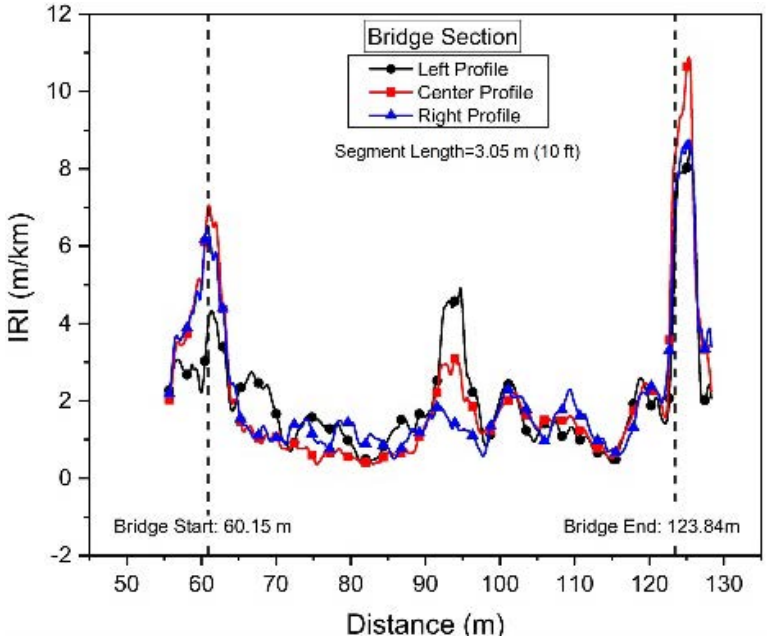

Source: FHWA.
1 m = 3.28 ft; 1 m/km = 5.28 ft/mi.

B. Bridge section.

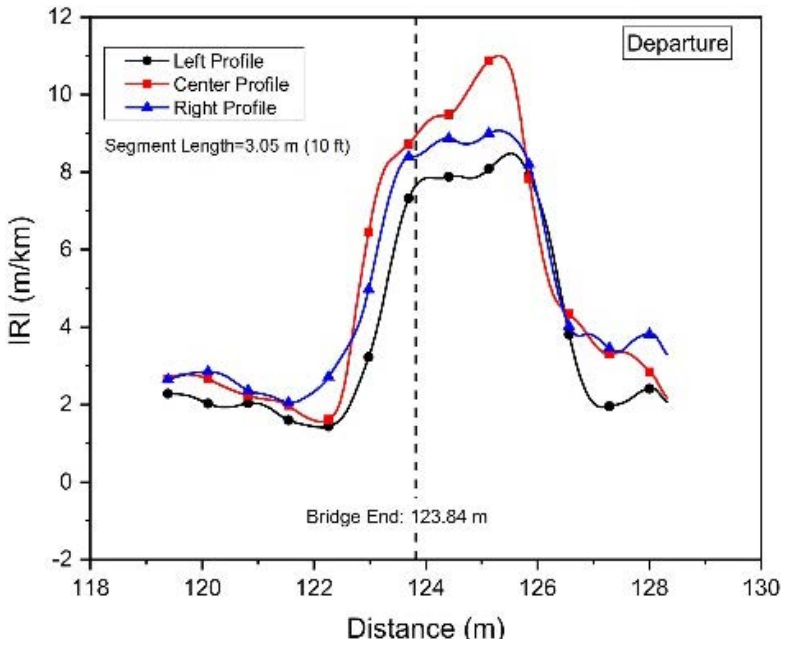

Source: FHWA.
1 m = 3.28 ft; 1 m/km = 5.28 ft/mi.

C. Departure section.

Figure 2. Graphs. IRI analysis with 3.05-m (10-ft) segment length for a Skew_Conv abutment.

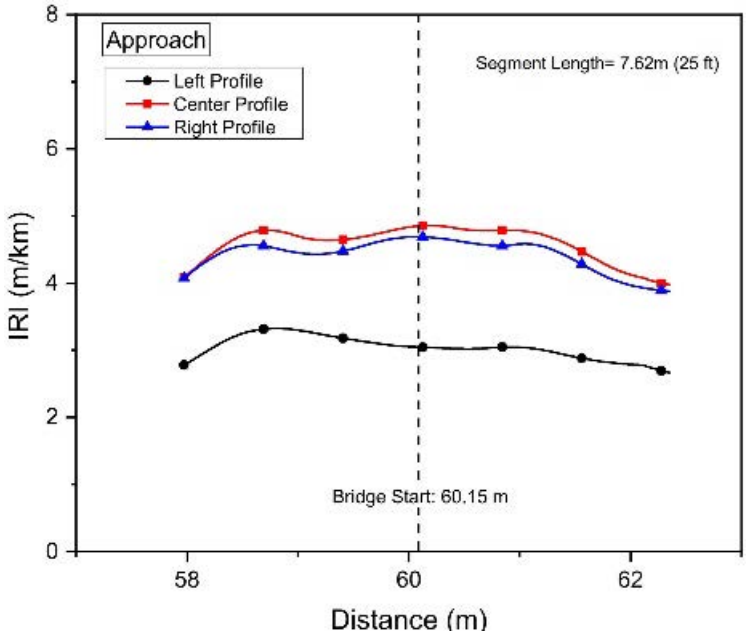

Source: FHWA.
1 m = 3.28 ft; 1 m/km = 5.28 ft/mi.

A. Approach section.

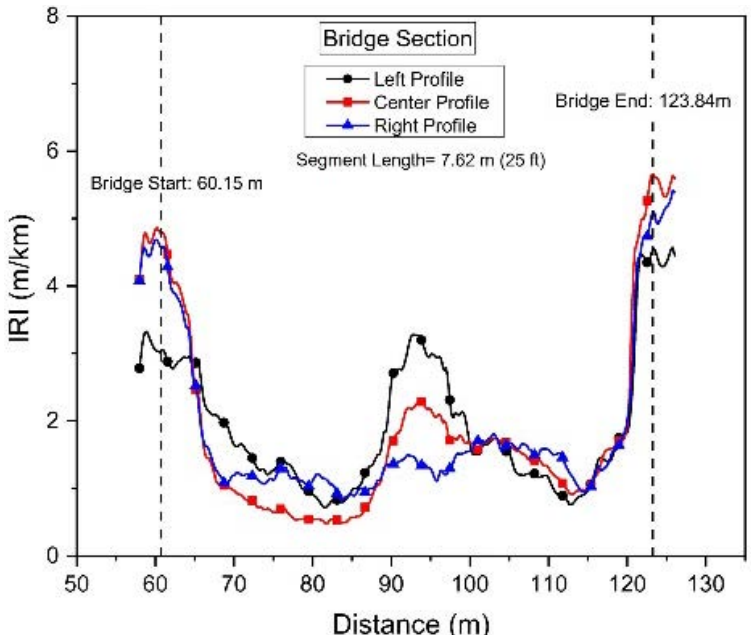

Source: FHWA.
1 m = 3.28 ft; 1 m/km = 5.28 ft/mi.

B. Bridge section.

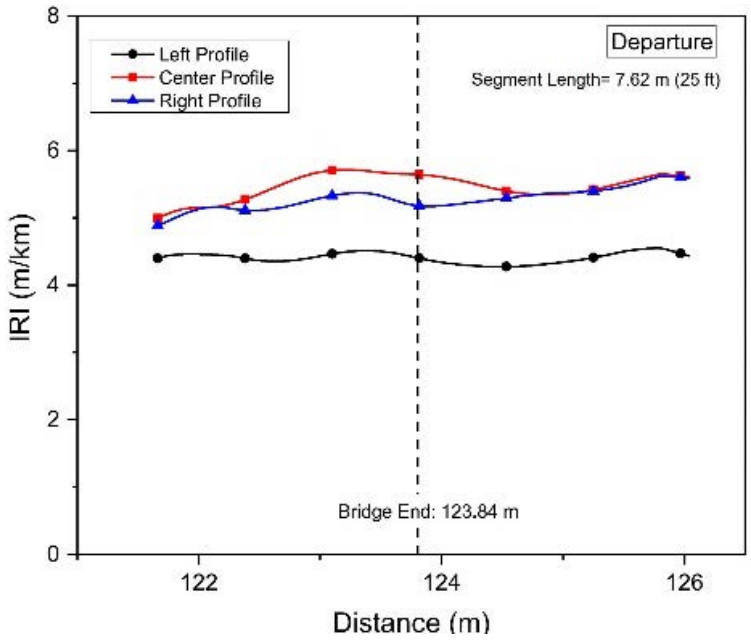

Source: FHWA.
1 m = 3.28 ft; 1 m/km = 5.28 ft/mi.

C. Departure section.

Figure 3. Graphs. IRI analysis with 7.62-m (25-ft) segment length for a Skew_Conv abutment.

The first point to notice from figure 1 through figure 3 is that the calculated IRI value decreases significantly as the segment length increases. For a segment length of 0.31 m (1 ft), the scale of

the *y*-axis peaks at 35 m/km (184.8 ft/mi), whereas for a segment length of 7.62 m (25 ft), the scale ranges up to only 8 m/km (42.24 ft/mi). The start and end points of the bridge (marked by dashed vertical lines in figure 1-B, figure 2-B, and figure 3-B) show clear spikes in the IRI trace, indicating a local roughness encountered by the inertial profiler. This spike tends to diminish as the segment length is increased. Because there is no standard recommended segment length for quantification of bridge approach roughness, further analysis on the effect of these different segment lengths was warranted. This would ensure selection of the most appropriate segment length for analysis of all the bridge approach profiles. Considering the scale of the problem being investigated (i.e., BEB), a shorter segment length would appear to be more appropriate. Based on the IRI traces in figure 1 through figure 3, it was apparent that using the 7.62-m (25-ft) segment length would not be beneficial for the current research effort. The differences between the 0.31- and 3.05-m (1- and 10-ft) segment lengths were not as apparent from the initial comparisons. Therefore, it was decided to further investigate this matter to select the most appropriate segment length.

Another interesting observation from the profile data presented in figure 1 through figure 3 is that the IRI trace showed an upward spike near the midspan of the bridge section. This spike is a reflection that this specific bridge has two spans with a center support. As seen from figure 1 through figure 3, although the spike is recorded by all three segment lengths, its magnitude is much clearer for the shortest segment length (0.31 m [1 ft]). Although the goals of this research do not include analysis of the bridge deck's roughness, acknowledging this phenomenon is important because it demonstrates another advantage of using inertial profilers to identify differential settlement and joint locations.

To compare the overall IRI values of each section of a bridge profile and the IRI values as the segment length increases from 0.31 to 3.05 m (1 to 10 ft), the maximum values calculated for each section using each segment length were plotted (figure 4). Figure 4-A shows the IRI values calculated using the 0.31-m (1-ft) segment, whereas figure 4-B shows the data for the 3.05-m (10-ft) segment for the same bridge data presented in figure 1 through figure 3.

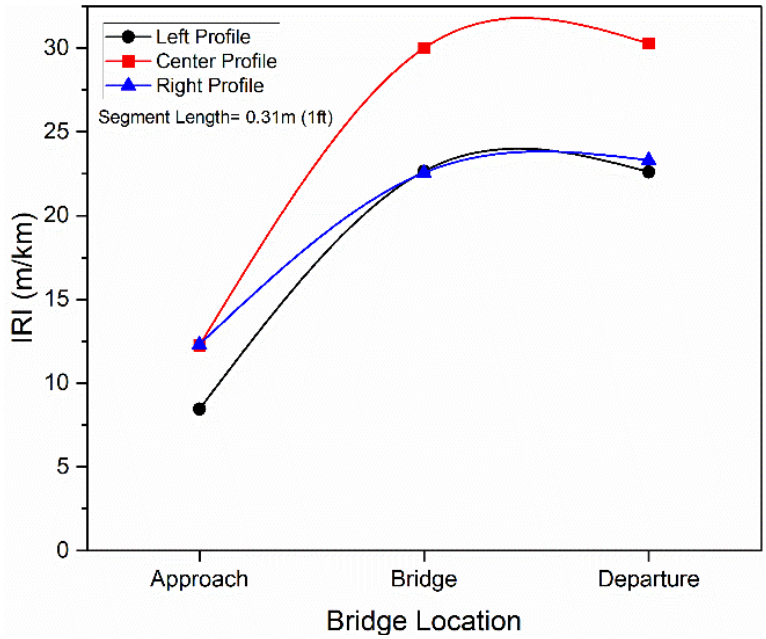

Source: FHWA.
1 m/km = 5.28 ft/mi.

A. 0.31-m (1-ft) segment length.

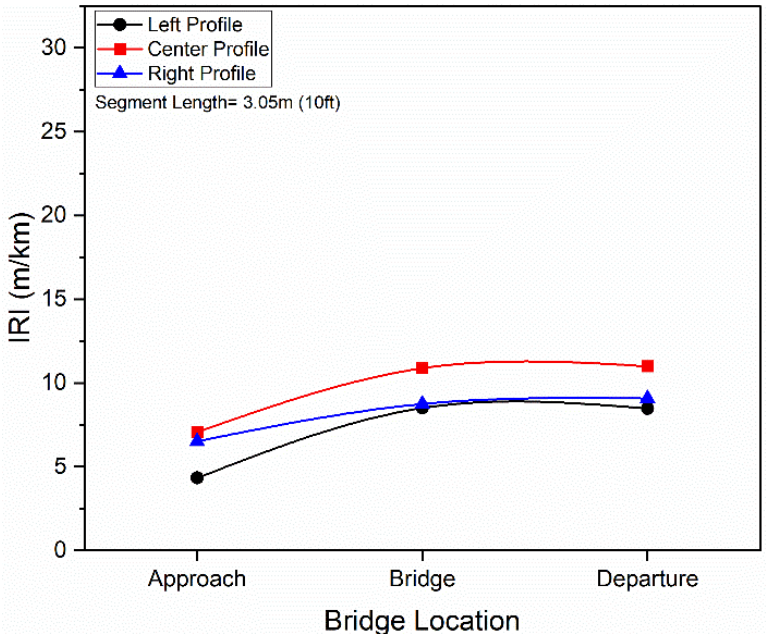

Source: FHWA.
1 m/km = 5.28 ft/mi.

B. 3.05-m (10-ft) segment length.

Figure 4. Graphs. IRI values versus segment length trends for a Skew_Conv abutment.

Visually, the trend of the IRI values with the change in segment length is relatively consistent; the primary difference is the IRI values themselves. The decrease in IRI value with increasing segment length can be attributed to the amount of information being filtered out with the larger

segment length. The two segment lengths in figure 4 correspond to moving average windows of 0.31 m (1 ft) and 3.05 m (10 ft). When larger segment lengths are used, extreme high or low values are omitted because of the smoothing effect of the moving average. Such omissions may not be problematic on long pavement sections, but using larger segment lengths may not be ideal when local quantification of surface roughness is of importance (as in this study). Hence, although a segment length of 7.62 m (25 ft) may be appropriate for roughness quantification of long pavement sections, it is not suitable when comparing the local roughness at bridge approach sections.

It is also important to note that unlike figure 4, changes in segment length can sometimes also result in changes in the relative IRI values for the approach, bridge, and departure sections. For example, figure 5 presents similar data as figure 4 for a Skewed GRS (Skew_GRS) abutment. As expected, increasing the segment length from 0.31 m (1 ft) to 3.05 m (10 ft) results in significantly lower IRI values. This segment length increase also results in a change in the relative magnitudes of the left, center, and right profile IRI values.

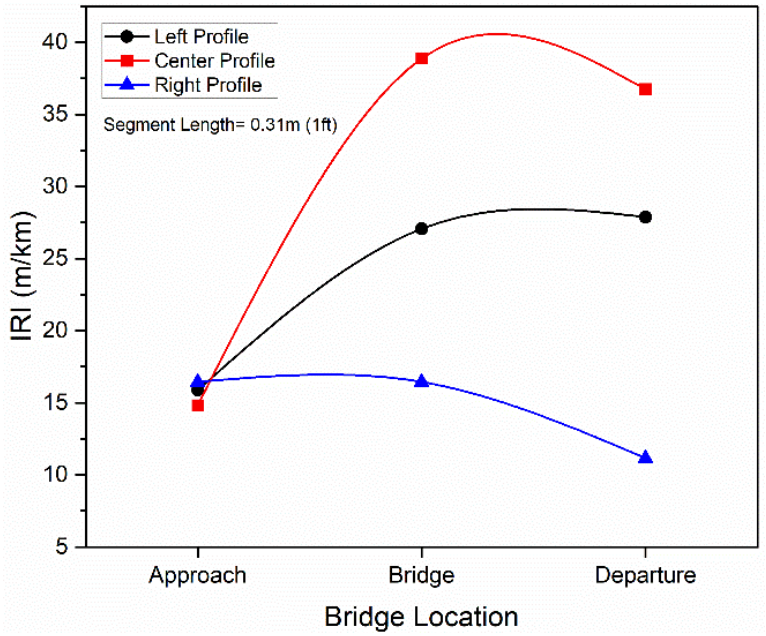

Source: FHWA.
1 m/km = 5.28 ft/mi.

A. 0.31-m (1-ft) segment length.

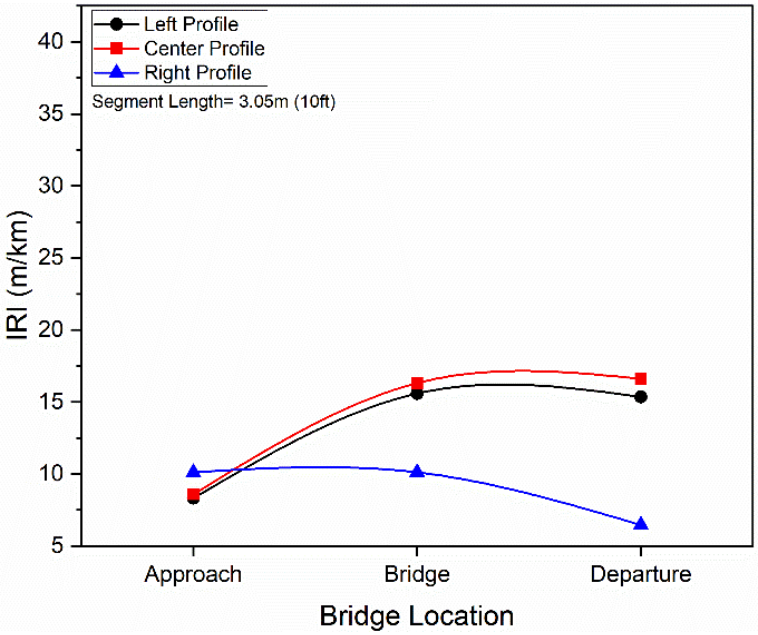

Source: FHWA.
1 m/km = 5.28 ft/mi.

B. 3.05-m (10-ft) segment length.

Figure 5. Graphs. IRI values versus segment length trends for a Skew_GRS abutment.

Another example, presented in figure 6, shows how changing the segment length can lead to a complete change in the shape of the maximum IRI trace going from the approach section to the bridge to the departure section (note how the shape of the trace for the center profile in figure 6-A is different from that in figure 6-B). The cause of the change in shape is unknown. The data presented in figure 6 correspond to a bridge with a Perpendicular GRS-IBS (Perp_GRS) abutment.

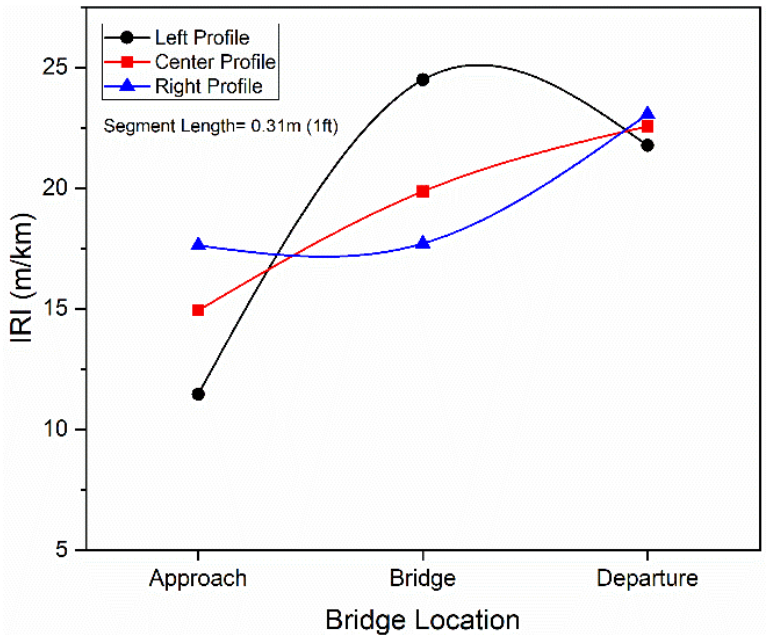

Source: FHWA.
1 m/km = 5.28 ft/mi.

A. 0.31-m (1-ft) segment length.

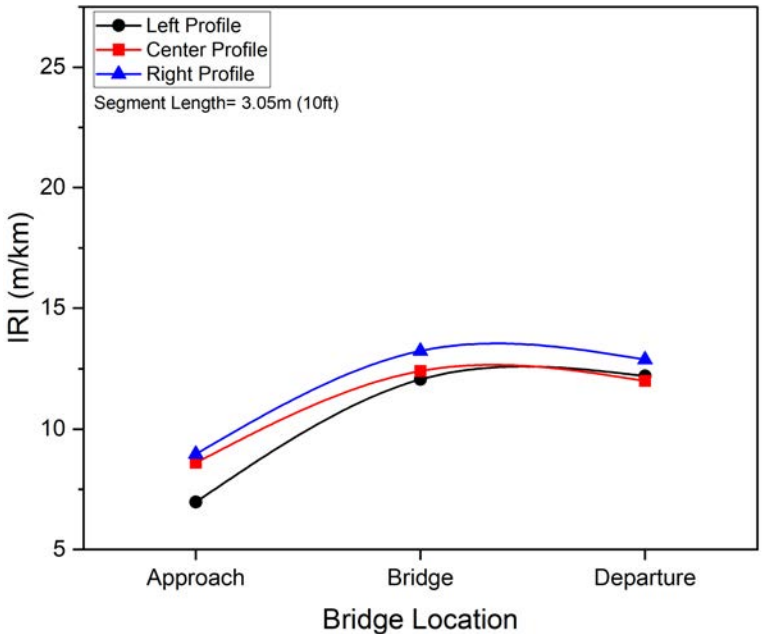

Source: FHWA.
1 m/km = 5.28 ft/mi.

B. 3.05-m (10-ft) segment length.

Figure 6. Graphs. IRI values versus segment length trends for a Perp_GRS abutment.

To compare all maximum IRI values for all bridges and segment lengths within this study, a scatterplot is presented in figure 7. Note that the *x*-axis in figure 7 represents "profile number" (i.e., the index of a profile measurement without distinguishing between approach and departure

sections). For example, considering a particular bridge structure and a particular direction of travel, profile number 1 would represent the data from the approach section, whereas profile number 2 would represent the data from the departure section. Multiple passes in one direction were combined to calculate one representative profile (this approach has been used for the entirety of this report). As seen from figure 7, the points corresponding to a segment length of 0.31 m (1 ft) had consistently higher maximum IRI values than the points corresponding to the other two segment lengths. The points corresponding to a segment length of 7.62 m (25 ft) recorded the lowest maximum IRI values. It is important to note that this comparison was performed by treating data in both directions of travel as separate datasets. This was justified because some bridges were not connected at the centerline of the road and therefore could essentially be treated as individual structures.

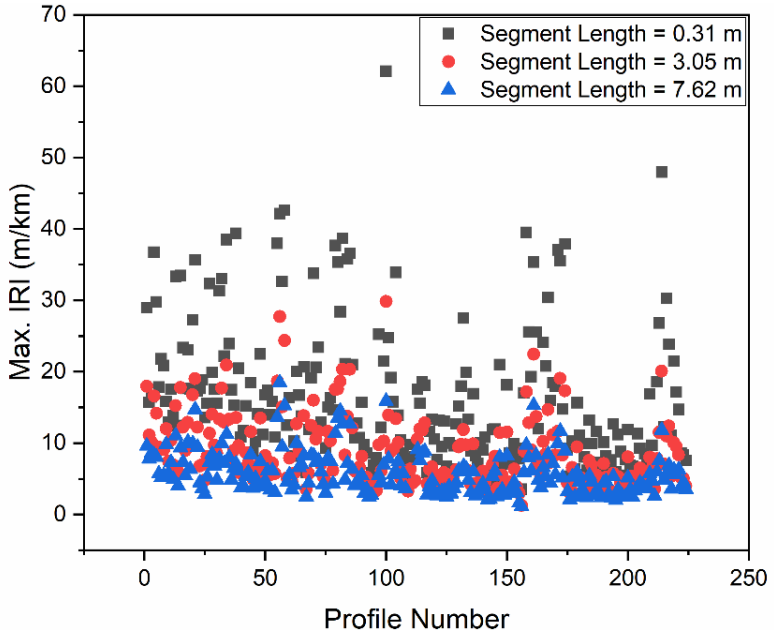

Source: FHWA.
1 m = 3.28 ft; 1 m/km = 5.28 ft/mi.

Figure 7. Graph. Scatterplot of maximum IRI values for approach and departure sections (combined) based on segment length.

The inertial profiler used to collect the provided data had a set sample interval of 23.9 mm (0.9 inch). Using the 0.31-m (1-ft) segment length has the benefit of analyzing the localized roughness of a section at a much higher resolution. Although some useful information can still be obtained from IRI calculations using a 3.05-m (10-ft) segment length, the research team decided that using the IRI values calculated using a 0.31-m (1-ft) segment length would provide the most details to adequately compare the BEB magnitudes for different bridges.

Rolling Straightedge

The second method used to quantify the roughness of the localized BEB approach for the 66 bridges in the dataset for this project was the RSE deviation method. The RSE measurement process detects the deviations of surface elevation along the road profile from a reference line. When RSE measurements are collected in the field, they are generally collected using a device

with a straightedge approximately 3.05 m (10 ft) long mounted onto wheels. The device is guided along the pavement, and deviations are measured from the centerpoint of the straightedge (Sayers and Karamihas 1998). RSE analyses performed in ProVAL were completed assuming that the straightedge length was 3.05 m (10 ft) based on the specifications of an RSE device, according to Henderson et al. (2016). Results from an RSE analysis are commonly displayed graphically, as shown in the example in figure 8.

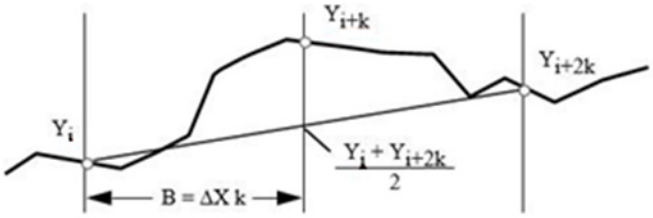

Y_i = ith profile elevation; B = base length; ΔX = distance interval;
k = an integer parameter for the filter.

Figure 8. Graph. Geometric view of an RSE output (Sayers and Karamihas 1998).

Figure 9 shows the graphical results of the RSE analysis for a bridge with a Perpendicular-Conventional (Perp_Conv) abutment. The graphical representation of the data clearly indicates some locations along a bridge profile that are more problematic than others. By looking only at the profile shown in figure 9-A, the results appear to have small deviation values. By looking at the profiles in figure 9-B (bridge section) and figure 9-C (departure section), a better picture of the surface profile roughness along the length of the bridge can be obtained. Although the approach section appears to be relatively smooth, there is an obvious bump at the departure section of this bridge.

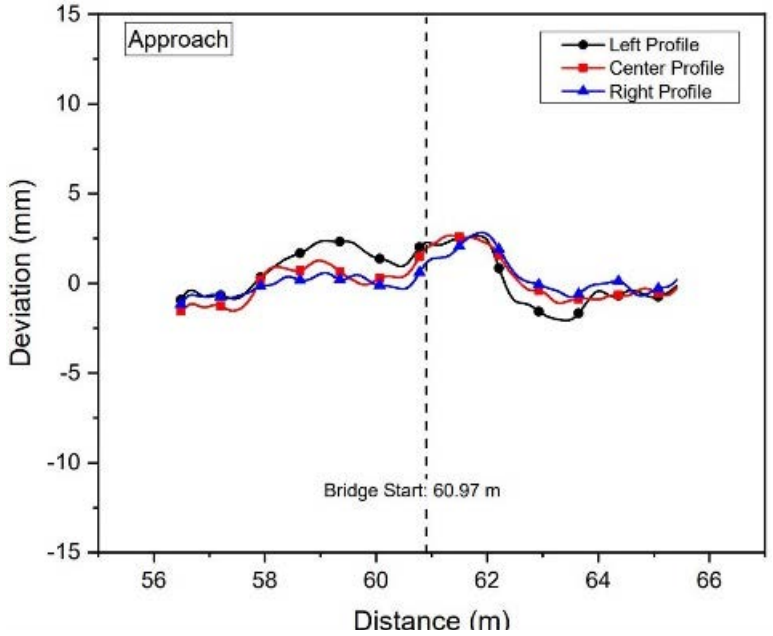

Source: FHWA.
1 m = 3.28 ft; 1 m/km = 5.28 ft/mi.

A. Approach section.

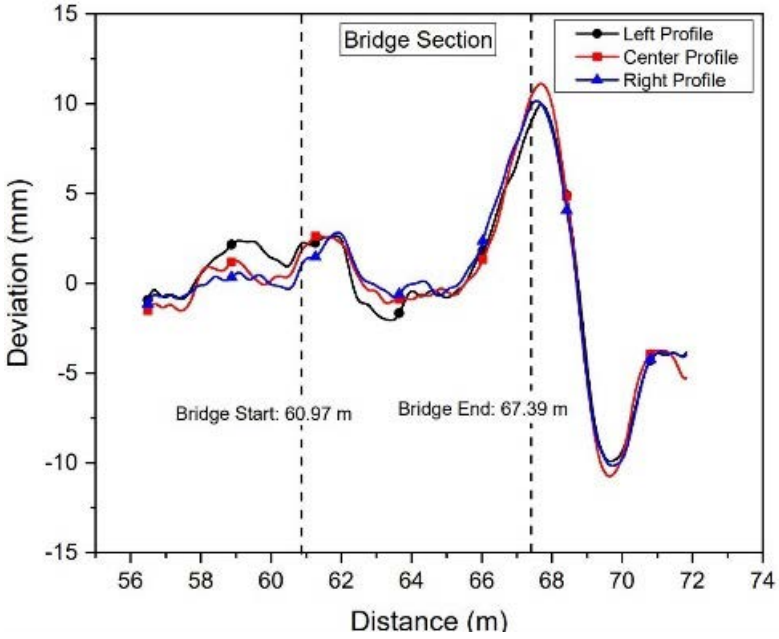

Source: FHWA.
1 m = 3.28 ft; 1 m/km = 5.28 ft/mi.

B. Bridge section.

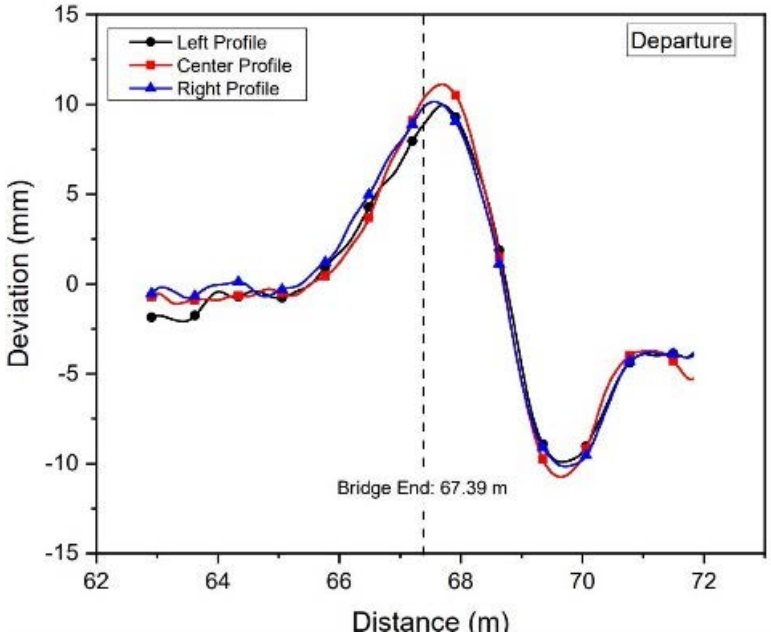

Source: FHWA.
1 m = 3.28 ft; 1 m/km = 5.28 ft/mi.

C. Departure section.

Figure 9. Graphs. RSE deviation traces for a Perp_Conv abutment.

As stated in the previous section, IRI is the most commonly used concept to quantify surface profile roughness for pavements. However, as already illustrated, IRI values are greatly dependent on the segment length selected during analysis. Accordingly, to ensure that no important information was lost in the data analysis due to use of an inadequate segment length, this research effort also analyzed each surface profile using the RSE deviation method. Data analysis presented in subsequent sections of this report will primarily focus on IRI values calculated using a 0.31-m (1-ft) filter length as well as the maximum and minimum deviations obtained from RSE analyses.

DESCRIPTION OF DATASET OBTAINED FROM FHWA

To support the decisions made regarding the use of the IRI settings, segment lengths, and RSE settings in this project, details of the data obtained through a separate FHWA data collection effort are included in this section. Based on the procedures detailed in the *ProVAL User's Guide* (The Transtec Group 2016) and from Henderson et al. (2016), the provided data were evaluated in the most congruent fashion. These decisions involved the following considerations: direction of travel, lane location, and number of passes recorded in each direction.

In addition to the characteristics provided in the raw data files used for this project, additional details evaluated were the abutment type (GRS or conventional) and the bridge geometry (perpendicular or skewed abutment). Pertinent details were defined for each bridge in a collective list and included the following:

- State.
- Testing identification (ID).
- City/county.
- Bridge ID.
- Bridge geometry.
- Bridge type.
- Testing date.
- Latitude/longitude.
- Direction.

The State and testing ID details were used to categorize the results in all tables in this report. These details, along with the direction of travel, relate to the file names provided in the data collection spreadsheet and are explained in further detail in the next paragraph. One feature of interest in the analysis of this project was the bump magnitude corresponding to different bridge geometry and abutment configurations. For any statistical analysis effort, a balanced dataset is usually desired. In other words, the data should have equal representation of different factors being studied. This aspect is further discussed in the Distribution of Available Data by State section of this report. The testing date information was used to categorize the bridge age based on the time between the construction and the testing of the structure. The final feature addressed in the collective list was the latitudinal and longitudinal coordinates of the bridge location. This information was beneficial to compare to the location included in FHWA's Long-Term Bridge Performance (LTBP) web portal, LTBP InfoBridge™ (FHWA 2019). The InfoBridge database was used to collect information on each bridge, including bridge length, date of original construction (i.e., age), average daily traffic (ADT), and number of freeze/thaw cycles per year. All these characteristics were used in the statistical analysis stage of this study and can be found in subsections of the Analysis of Inertial Profiler Data and Groupings chapter of this report.

The State, testing ID, and direction of travel are directly related to the naming convention of the raw data files provided for this study. Each profile provided was saved as an individual file with an SSNNNDLV naming convention; according to Henderson et al. (2016, p. 18), the acronym is defined as follows:

- SS: State in which site is located. Long-Term Pavement Performance (LTPP) standard agency codes are used (e.g., 36 for New York).

- NNN: Bridge identification (ID). This is a numeric character to identify the bridge as tested in sequence…

- D: Letter code defining direction of travel (e.g., N for north, S for south, W for west, or E for east).

- L: Profile lane (i.e., lane 1, 3, 5, 7, 9, etc. in the positive direction and 2, 4, 6, 8, etc. in the negative direction taken from the median or centerline).

- V: Sequential visit identifier that indicates the visit code for the current profile data collection. This identifier indicates the number of times a set of profile runs has been

collected at a site since the site was first profiled. An appropriate letter should be used for the current profiling (i.e., A used for the first visit, B for the second visit, etc.).

The collective list category of testing ID is the same information as the bridge ID category explained in the acronym naming convention. The bridge ID category in the collective list denotes the National Bridge Inventory number, which can be found in LTBP InfoBridge.

For each file, the pass number was added at the end of the file name using the format SSNNNDLV.P##. The following are examples of this nomenclature for data specific to this project:

- 30001N1A.P01—bridge located in Montana (30), the first bridge profiled (001) in the northbound direction (N), the lane is the positive outer lane (1), data collected during the first visit (A) and from the first pass (P01).

- 39024E1A.P02—bridge located in Ohio (39), the 24th bridge profiled (024) in the eastbound direction (E), the lane is the positive outer lane (1), data collected during the first visit (A) and from the second pass (P02).

All bridge profile data were for only one lane in each direction, except for two bridges (UT 1 and UT 2) that also provided profile data for a second lane in the same direction of travel. For this reason, there was inconsistency in the tabular data found in appendix A through appendix C. The locations where multiple lane data were provided have been included in separate tables within each appendix to avoid confusion. In terms of the direction of travel and the lane location, each was considered as a separate structure, resulting in 112 profiles for 66 bridges. Note that the number of profiles is not equal to twice the number of bridges. Although it would have been preferable to analyze all structures in both directions, there were bridge locations for which profiler data were collected in only one direction.

Although the decision to analyze each direction as separate profiles was not a consistent possibility, it was a necessary step. Upon reviewing maps of the bridge locations within ProVAL, it was discovered that not all bridges were connected at the median. Because of the separate structures in different directions of travel, it could not be assumed that the bridge would behave as a monolithic structure; therefore, it was considered as two separate structures for surface profile analysis efforts.

Figure 10 displays the profile collected for a bridge not connected at the center median as well as one that had data collected in two specified lanes in each direction. Just by observing the shape of a highway or interstate, differences in the profile can be seen in the inside and outside lane with respect to the median. Because of the incongruous use of lanes, the roadway potentially breaks down differently, resulting in distinct profiles in each lane.

Original Map: © 2020 Microsoft® Bing. Map modifications: FHWA.

Figure 10. Photo. Aerial photo of a bridge structure analyzed.

The next detail in the profiler data considered in the process was the number of passes collected for each bridge. Adding the pass number to each file was a key component in the cross-correlation process, explained more in the Cross-Correlation Analysis section. In general, the cross-correlation measurements were performed to ensure the data from multiple passes for each bridge and direction combination were repeatable. To perform this measurement, more than one pass had to be collected for any combination. The base profile used to compare all additional passes was always selected as the first pass number collected (mainly P01 with occasional later passes). This detail is significant when reviewing the profile data because the dataset did not include the first pass (P01) for every bridge and direction combination. The number of passes provided in the data varied between one and five, and the multiple passes did not always appear in consecutive order.

Along with its impact on the cross-correlation measurement process, the number of passes affected the presentation of the IRI and RSE plots created to display the analysis results. As previously stated, the cross-correlation process requires more than one pass to complete. Irrespective of whether there were two or five passes, the plots and analyses were performed based on the average results for IRI and RSE calculations. The only time the data were presented separately for each pass was for the cross-correlation values. As seen in table 2 and appendix B, cross-correlation values for each pass are presented either as a range of the maximum values or as the results of each pass individually.

The next step taken to organize and process the data was to segment the bridge profiles into three sections: approach, bridge, and departure. This process is explained in further detail in the following section.

DEFINING BRIDGE APPROACH AND DEPARTURE SECTIONS

Part of the analysis process for the bridge profiles was determining the locations of rough spots and related bump issues along the bridge, primarily in the approach and departure sections. One of the objectives of this study was to identify whether approach sections in bridges were more

likely to have greater bump problems than departure sections, or vice versa. Each bridge profile was divided into three sections: approach, bridge, and departure. Based on the procedure used by Henderson et al. (2016), a distance of 6 m (19.7 ft) was added to either side of the start and end of the bridge deck (identified by marker flag placements in the analysis software), as shown in figure 11.

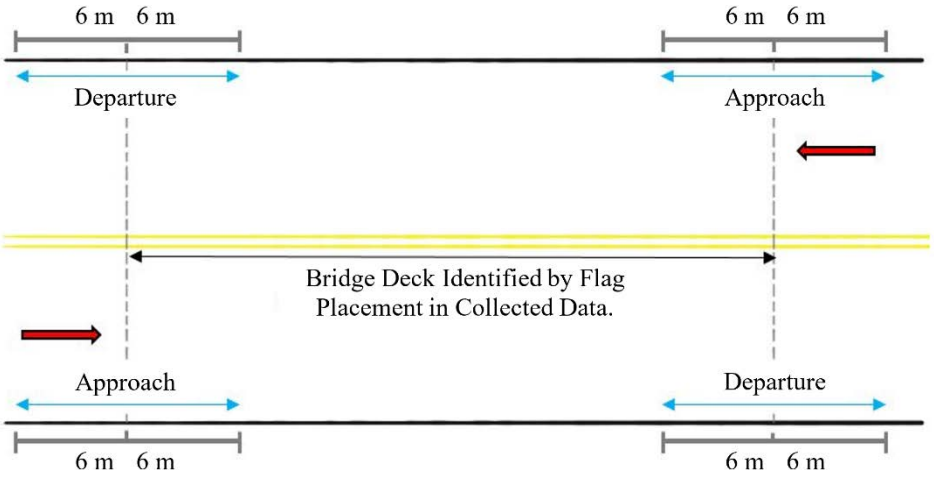

Source: FHWA.
1 m = 3.28 ft.

Figure 11. Illustration. Approach, bridge, and departure section diagram.

Figure 11 depicts the layout of the approach, bridge, and departure sections used for most of the bridges analyzed. Note that the approach and departure sections are aligned with the direction of traffic in each respective lane. Using the approach and departures sections of the profile, analysis was performed on roughness and bump occurrences related to the transition area onto and off the bridge deck. This general process worked well for most of the bridges analyzed; however, it created issues for bridges shorter than 6 m (19.7 ft). Although FHWA does not consider structures with span lengths less than 6.1 m (20 ft) along the centerline as bridges (FHWA 2004), this report considers all analyzed structures as bridges, regardless of length.

If the same process depicted in figure 11 is used for bridges shorter than 6 m (19.7 ft), the section marked as “approach” would overlap into the departure section of the bridge, making it impossible to differentiate between the bridge approach and departure sections. This issue is illustrated in figure 12; the overlap that occurs for bridges shorter than 6 m (19.7 ft) produces duplicate data for the approach and departure sections.

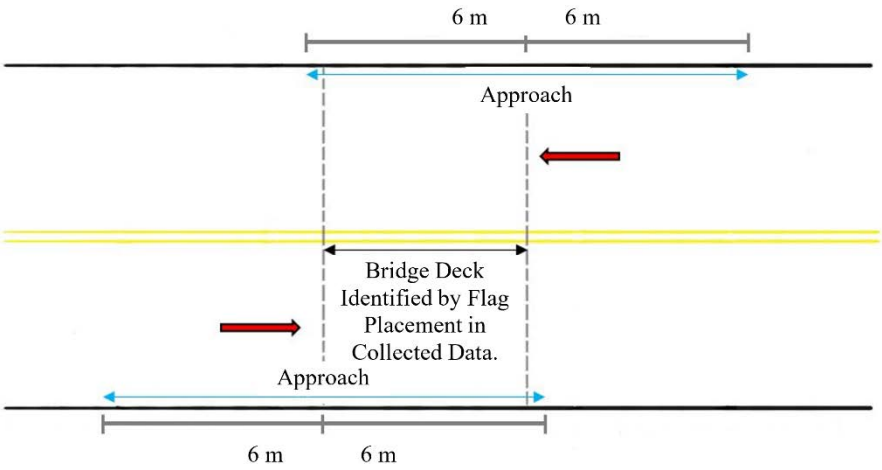

Source: FHWA.
1 m = 3.28 ft.

Figure 12. Illustration. Approach section overlap diagram.

To work around this problem, the distance added before and after the start of the bridge deck (identified by a reflective trigger during the data collection) was changed from 6 m (19.7 ft) to a length equal to one-half the bridge length. Note that temporary reflective triggers are placed at various locations along the roadway, including the start and end of the bridge deck as well as a defined location to initiate data collection by the profiler. As described in further detail in the Analysis of Inertial Profiler Data and Groupings section, the first reflective trigger appears 61 m (200 ft) before the start of the bridge and the final trigger appears 61 m (200 ft) after the end of the bridge deck. The first and final reflective triggers allow calibration of the instrumentation on the vehicles. These trigger locations are represented as flags within ProVAL (Henderson et al. 2016). This method was applied to all bridges equal to or shorter than 6 m (19.7 ft).

The final method for analyzing the sections of shorter bridges used a combination of the two previous methods: adding 6 m (19.7 ft) before and after the bridge deck and adding one-half the bridge length to the deck side of each joint. This process is depicted in figure 13.

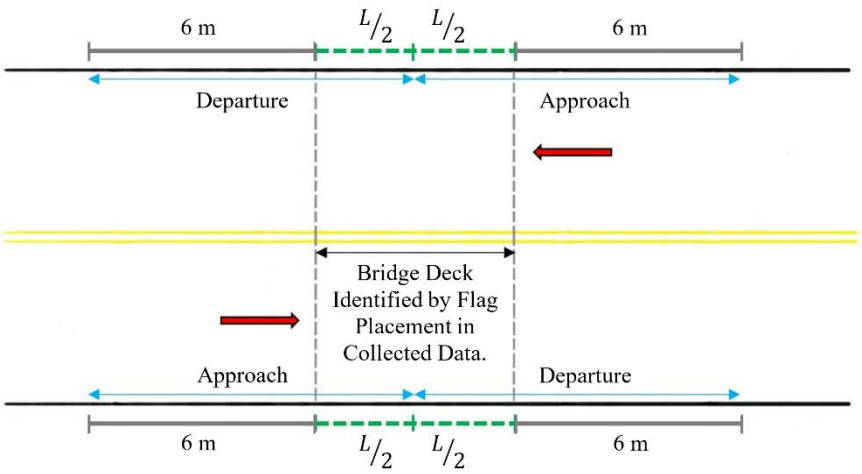

Source: FHWA.
1 m = 3.28 ft.
Note: $L/2$ is equal to one-half the bridge length.

Figure 13. Illustration. Final method for determining approach, bridge, and departure sections for bridges shorter than 6 m (19.7 ft).

The final method for determining the approach and departure sections was used to provide data for most of the bridges that were shorter than 6 m (19.7 ft). Of the 112 bridge profiles provided, 14 were less than 6 m (19.7 ft) across the bridge deck, requiring this alternative method of determining sections. An additional issue occurred with the shortest of these bridges. The two shortest bridges evaluated were a Skew_GRS abutment with an approximate length of 3.24 m (10.6 ft) and a Perp_GRS abutment with an approximate length of 3.01 m (9.88 ft). Using the final method proposed in figure 13, no data were provided for the IRI measurement with the 7.62-m (25-ft) segment length because the total length of the approach and departure sections would be 7.60 m (24.9 ft) for the Skew_GRS abutment and 7.50 m (24.6 ft) for the Perp_GRS abutment. Although these values are not far from the 7.62-m (25-ft) segment length, any section less than the segment length would not provide results. Nevertheless, the research team decided not to alter the methods used to define the approach and departure sections of each bridge any further to avoid confusion during the final data analysis. For this analysis, the research team decided not to focus on IRI calculations with a segment length of 7.62 m (25 ft).

CHAPTER 2. CHECKING THE OVERALL DISTRIBUTION OF THE PROFILER DATA

Once all the profile data were reduced and the values of maximum IRI (for a segment length of 0.31 m [1 ft]) and maximum and minimum RSE deviations were established for each approach and departure section, the next step involved selecting an appropriate method to analyze the dataset to study the effects of different factors on approach/departure roughness. It should be noted that the measurements of minimum and maximum RSE deviations denote the displacement above and below a hypothetically smooth (i.e., horizontal) profile, respectively. Before selecting any statistical analysis procedure, it is important to investigate the overall distribution of the data to assess whether the data fit commonly observed distributions. Accordingly, the overall distributions of the maximum IRI values (for a segment length of 0.31 m [1 ft]), maximum RSE deviations, and minimum RSE deviations were checked. Figure 14-A through figure 14-C show the frequency distributions of the maximum IRI (for a segment length of 0.31 m [1 ft]), maximum RSE deviation, and minimum RSE deviation, respectively. Figure 14-A through figure 14-C also show standard normal distribution plots against the data and that the datasets are not normally distributed, which meant that some of the common statistical analysis methods that assume normal distribution had to be eliminated from consideration.

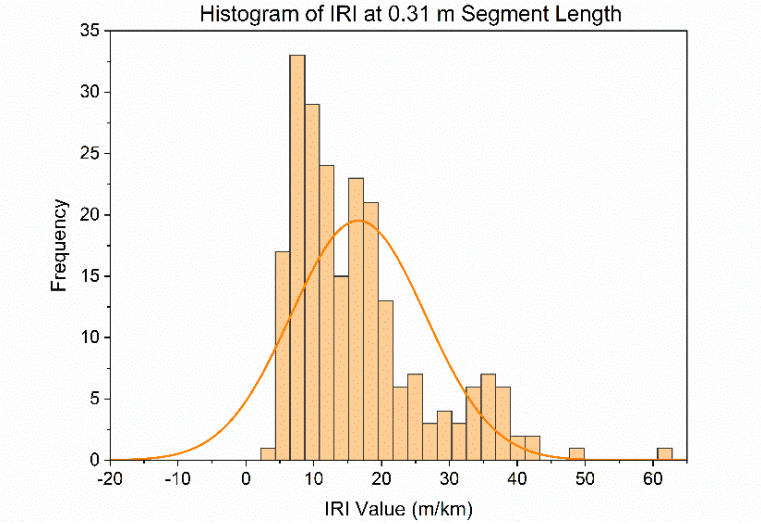

Source: FHWA.
1 m/km = 5.28 ft/mi.

A. Maximum IRI at 0.31-m (1-ft) segment length.

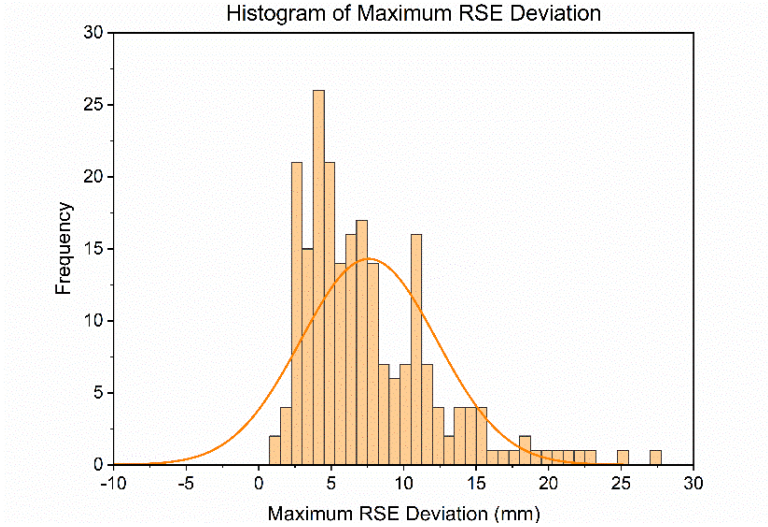

Source: FHWA.
1 mm = 0.039 inches.

B. Maximum RSE deviation.

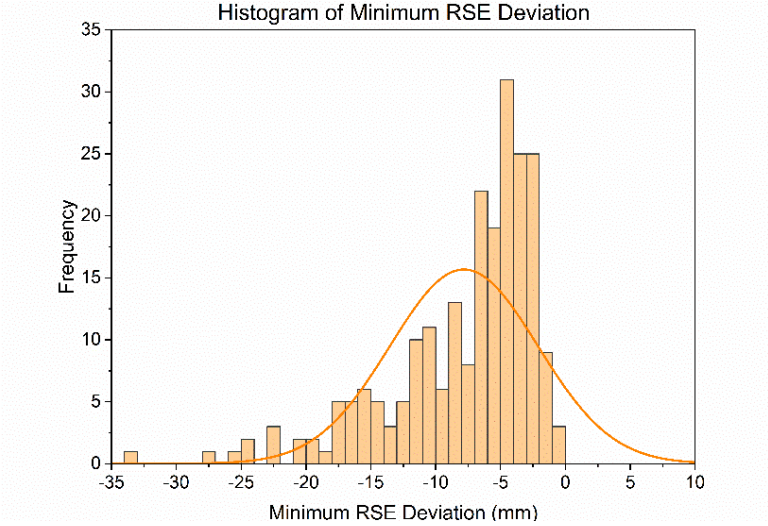

Source: FHWA.
1 mm = 0.039 inches.

C. Minimum RSE deviation.

Figure 14. Graphs. Frequency distribution for maximum IRI values and RSE deviations.

The fact that the three datasets are not normally distributed can also be illustrated through normal probability plots. Figure 15-A through figure 15-C show the normal probability plots for maximum IRI value (for a segment length of 0.31 m [1 ft]), maximum RSE deviation, and minimum RSE deviation, respectively. The circular symbols indicate the probability of data for IRI and RSE deviations, whereas the solid straight line is based on connecting the 25th and 75th percentiles of the data. If the circular symbols lay along the line, it would be acceptable to assume normality within the data, so these graphs also confirm that these data are not normally distributed. The research team therefore identified a data analysis tool that is insensitive to the distribution of the dataset being analyzed; the box and whisker plot method was selected in this

study because box plots are nonparametric in nature and display variation in samples of a statistical population without making any assumptions of the underlying statistical distribution (Ott and Longnecker 2015). The following section presents a brief background on box plots and how they should be interpreted.

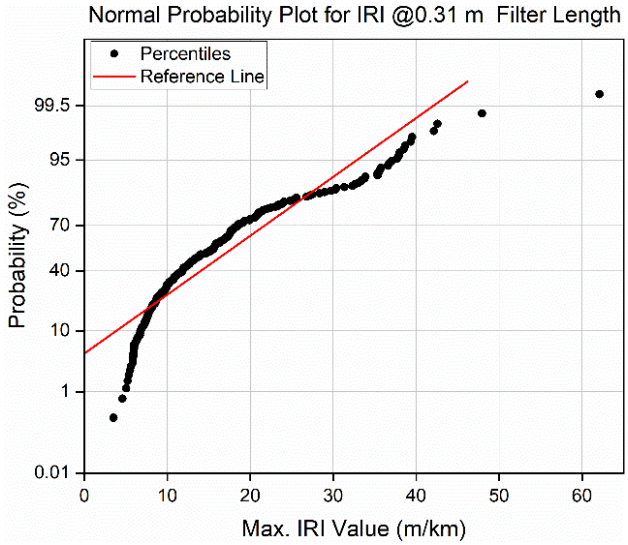

Source: FHWA.
1 m/km = 5.28 ft/mi.

A. Maximum IRI at 0.31-m (1-ft) segment length.

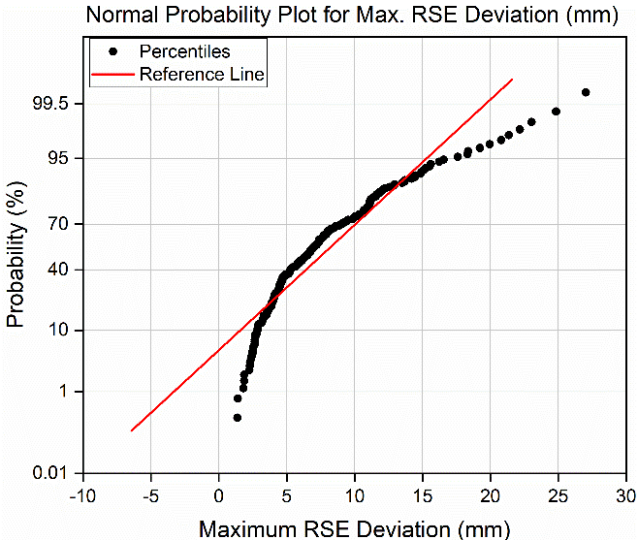

Source: FHWA.
1 mm = 0.039 inches.

B. Maximum RSE deviation.

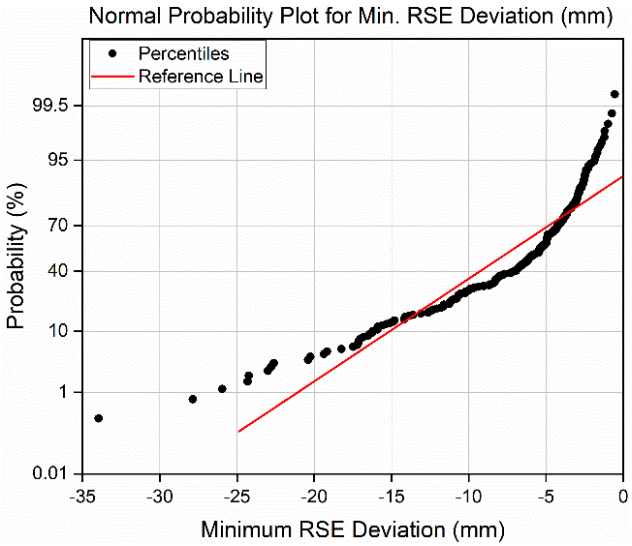

Source: FHWA.
1 mm = 0.039 inches.

C. Minimum RSE deviation.

Figure 15. Graphs. Normal probability plots for maximum IRI values and RSE deviations.

In addition to investigating the distribution of the data within the IRI and RSE measurements, a comparison of the data as they appear within each category was performed. These categories were bridge configuration, abutment type, bridge geometry, structure length, bridge age at the date of testing, ADT, and number of freeze/thaw cycles per year. Table 1 presents these categories along with the percent of each option per category. The information for these categories is based on the information found in LTBP InfoBridge. The thresholds were determined to ensure there were enough profiles in the dataset to perform the statistical analyses.

Table 1. Percent of profiles within each parameter considered during analysis.

Analysis Parameter	Total Profiles Considered	Possible Parameter Values	Profiles per Option	Percent of Total
Configuration	112	Perpendicular	64	57.1
		Skewed	48	42.9
Abutment type	112	Conventional	26	23.2
		GRS	86	76.8
Geometry	112	Perp_Conv	14	12.5
		Perp_GRS	50	44.6
		Skew_Conv	12	10.7
		Skew_GRS	36	32.1
Length	112	<15 m (49.2 ft)	62	55.4
		>15 m (49.2 ft)	50	44.6
Age	98	<5 yr	54	55.1
		>5 yr	44	44.9
ADT	98	<300	41	41.8
		>300	57	58.2
Freeze/thaw cycles per year	98	50–75	30	30.6
		>75	68	69.4

It should be noted that the categories of age, ADT, and number of freeze/thaw cycles per year have 98 profiles in each category whereas the other categories have 112 profiles. Because of how bridges are cataloged for State DOTs and FHWA, structures that are shorter than 6.09 m (20 ft) are not technically considered bridges (FHWA 2004). Of the 112 profiles included in the data for this project, 7 structures were shorter than this threshold. These 7 structures each had data in two directions, which accounts for the 14-profile deficit from the other categories listed in table 1.

BOX AND WHISKER PLOTS

The box and whisker plot is a tool in descriptive statistics where the overall distribution of the data is depicted with the use of quartiles (Ott and Longnecker 2015). In a typical box plot, the median value (50th-percentile value in the dataset) is represented as a horizontal line. A box around the median represents the interquartile range (IQR), or the range of values between the 25th-percentile data point and the 75th-percentile data point. The IQR indicates the range in which 50 percent of the data points occur, meaning 25 percent of the points occur below the bottom of the box and 25 percent of the points occur above the top of the box (Ott and Longnecker 2015). The dotted lines extending to horizontal bars above or below the box are known as whiskers. The end of a whisker is usually defined as the “inner fence” and is placed at a distance of 1.5 times the IQR from the end of the box (representing either the upper or lower quartiles at the top or bottom of the box, respectively). Any data point lying beyond the whiskers can be identified as an outlier. Figure 16 shows the components of a box and whisker plot representing a case where the median (Q2, value corresponding to the 50th percentile) lies at the middle of the distribution. In a skewed distribution, the median line will lie closer to either the Q1 (value corresponding to the 25th percentile) or the Q3 (value corresponding to the 75th percentile) line. While comparing two datasets, one can easily plot the box plots side by side and make inferences from the relative locations of the medians, the values of the IQR, the number of outliers, and so forth. The following sections use box and whisker plots to analyze the effects of different factors on bridge approach roughness as calculated using IRI (for a segment length of 0.31 m [1 ft]) as well as maximum and minimum RSE deviations. Moreover, for reader convenience, all box plots in this report have been labeled with the corresponding median values. Although the IQR values have not been separately labeled, they can be easily interpreted from the horizontal gridlines included in each plot. Note that in all subsequent discussions in this report, IRI values correspond to those calculated using a segment length of 0.31 m (1 ft).

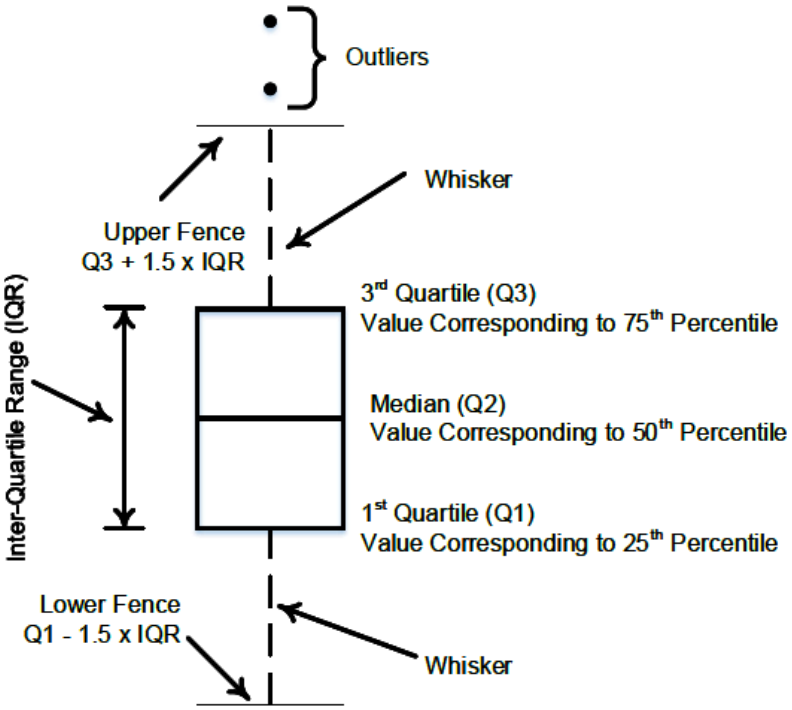

Source: FHWA.

Figure 16. Illustration. Components of a box and whisker plot.

COMPARING THE ROUGHNESS OF APPROACH AND DEPARTURE SECTIONS

After all the approach and departure sections were properly defined, the first task was to evaluate whether a distinct difference in pavement profiles existed between bridge approach and departure sections. To answer this question, the maximum IRI values for the approach and departure sections were compared for all bridges. The results are presented in figure 17, which shows the median values for the approach and departure sections were almost identical. Similarly, no significant difference exists between the IQR values. Based on the bridge profiles analyzed, no evidence was found to claim that the BEB is more or less severe at bridge approaches compared to bridge departures.

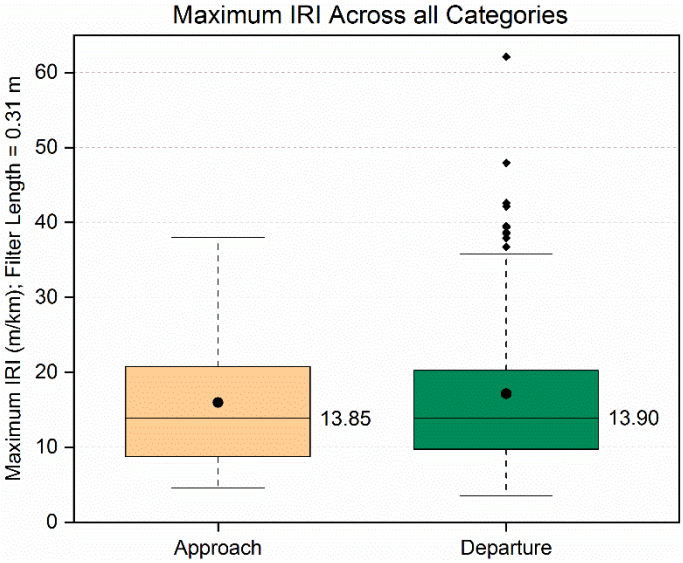

Source: FHWA.
1 m = 3.28 ft; 1 m/km = 5.28 ft/mi.

Figure 17. Graph. Maximum IRI values for approach and departure sections for all bridge types.

DISTRIBUTION OF AVAILABLE DATA BY STATE

There was an obvious imbalance in the types of bridge abutments analyzed in this dataset. Although there were bridges with conventional abutments and GRS abutments, these categories were not equally represented. In the complete list of bridges analyzed, only 15 bridges had conventional abutments, whereas 51 bridges had GRS abutments. Additionally, both abutment types were not consistently represented in each State for comparison. Ohio, for example, had 1 bridge with a conventional abutment tested and 26 with GRS abutments. The distribution of the abutment types by State can be seen in figure 18. Although the frequency of each abutment type was imbalanced, some of the States had both bridge types, which facilitated some form of comparison. However, 5 of the 14 States for which data were evaluated had only one type of abutment. New York was the only State for which data from multiple bridge abutments of different types were available (11 GRS abutments and 5 conventional abutments), so more direct comparison between the approach/departure roughness for the two bridge types was possible (presented in the Bridge Abutment Type section in this report). For this study, a conventional abutment represents the standard practice in the State/county, either before implementing GRS-IBS or in locations where an IBS is not suitable.

Further comparisons of the data available within each State included comparing the number of skewed versus perpendicular bridges; these data are presented in figure 19. Unlike the bridge abutment type, a relatively equal number of bridges within the dataset were skewed (28 bridges) and perpendicular (38 bridges). Like the abutment-type comparison, there was no consistency in which each State had both skewed and perpendicular bridges for this analysis. As a result, it was not possible to compare the performance of bridges based on abutment configuration within each State, but comparison as a group was possible. As seen from figure 19, the dataset from Ohio included 13 bridges with skewed abutments and 14 bridges with perpendicular abutments, which

facilitated the comparison between approach/departure roughness for perpendicular and skewed abutment bridges in Ohio (presented in the Bridge Configuration section).

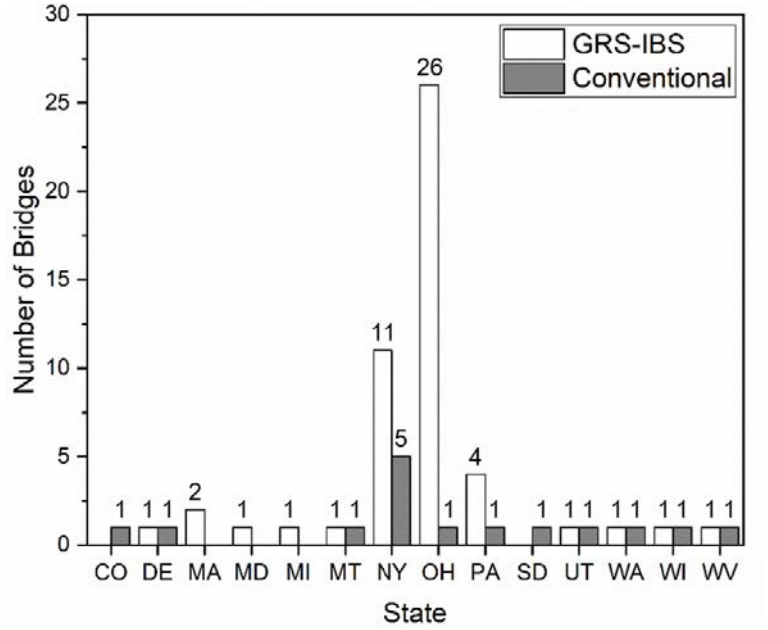

Source: FHWA.

Figure 18. Graph. Statewide distribution of GRS-IBS and conventional abutments in the available data.

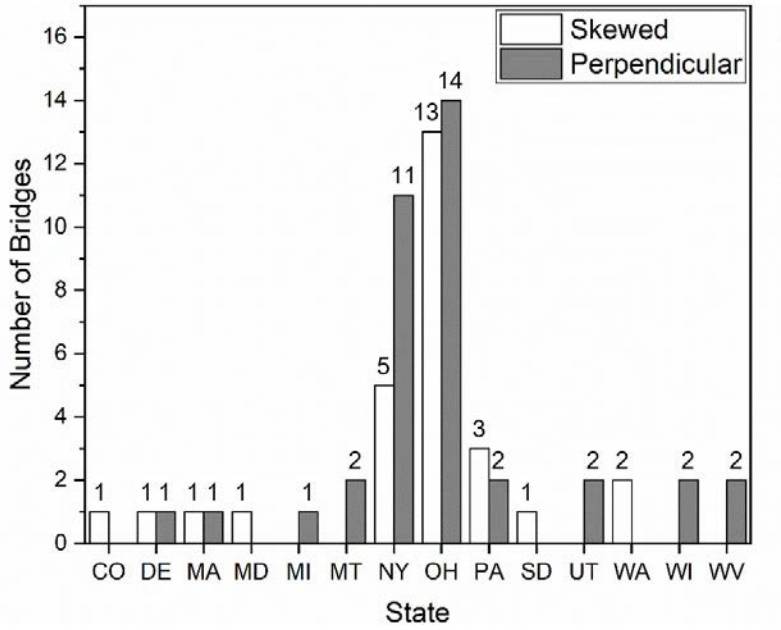

Source: FHWA.

Figure 19. Graph. Statewide distribution of perpendicular and skewed bridges in the available data.

GEOGRAPHIC REGIONS AND BRIDGE APPROACH AND DEPARTURE ROUGHNESS MEASUREMENTS

Statewide comparison of different bridge types was not possible within the available dataset because not all bridge types were represented in the data from individual States. To broaden the geographic comparison of the data, geographic regions defined within the LTPP database were used, as shown in figure 20 (FHWA 2019). Each bridge was categorized based on the geographic region in which it was located. The dataset comprised bridges within the North Atlantic (28 bridges), North Central (31 bridges), and Western (7 bridges) Regions. None of the bridges for which profile data were collected were in the Southern Region.

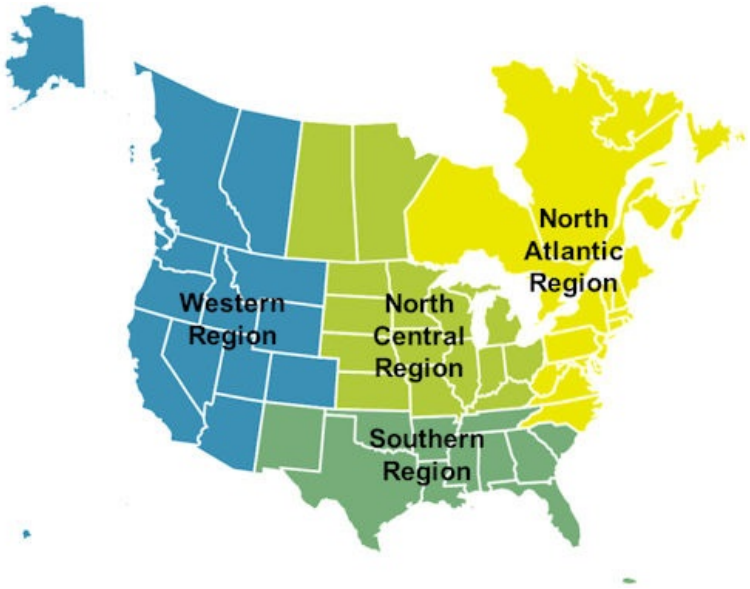

Source: FHWA.

Figure 20. Illustration. Map of different geographic regions defined in the LTPP database (FHWA 2019).

Using the LTPP geographic regions was appropriate because of their direct relation to pavement profiler data. Each region has a specific vehicle used for collecting pavement and bridge profile data. Comparing the bridges within each region minimizes correlation discrepancies that may occur between the vehicles used in different regions. Maximum IRI values for each region were compared for the 0.31-m (1-ft) segment length (figure 21). Maximum and minimum RSE deviations for each region were also compared (figure 22).

The results in figure 21 show that the lowest IRI values occurred in the North Atlantic Region. The highest median values, as well as the highest overall IRI values, occurred in the North Central Region. Generally, the median values were comparable between the three regions, with significant overlap of the IQR values (represented by the height of the boxes). This indicated no statistically significant difference between the samples, which was also checked using analysis of variance (ANOVA) (Ott and Longnecker 2015) (presented in the Checking the Statistical Significance of Different Factors on Bridge Approach/Departure Roughness section). The data corresponding to the Western Region had the smallest IQR as well as whisker lengths, possibly because data for only seven bridges were available from the Western Region, thereby limiting

the amount of scatter in the data. The data from the North Atlantic Region had several points lying outside the whiskers, indicating that most of the data points corresponded to low IRI values, thereby reducing the IQR value and whisker length. The several outlying points on the upper side of the IRI scale indicated that the data were skewed.

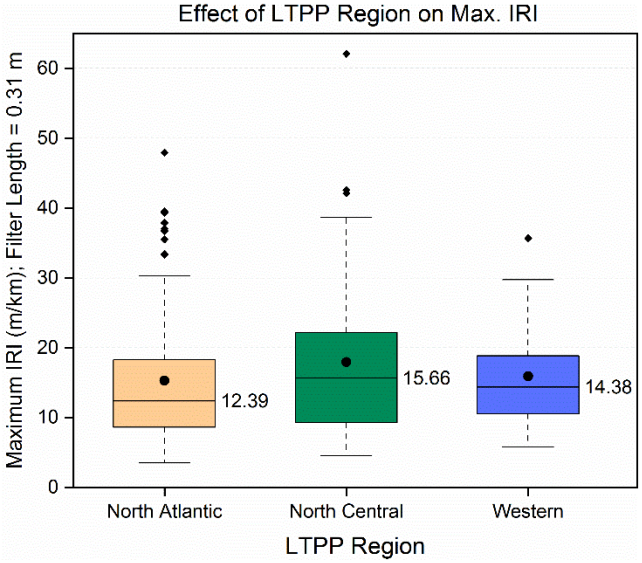

Source: FHWA.
1 m = 3.28 ft; 1 m/km = 5.28 ft/mi.

Figure 21. Graph. Maximum IRI values for 0.31-m (1-ft) segment length for approach and departure sections (combined) based on LTPP regions.

The results of the maximum and minimum RSE deviations for the LTPP regions in figure 22 show that the median values are relatively close to each other (like the IRI measurements). However, the relative values of the medians do not follow the same trend as the IRI plots. For example, in the RSE plots, the Western Region has the lowest median value, whereas in the IRI plot, the North Atlantic Region had the lowest median value. Nevertheless, based on both the IRI and RSE deviation plots, no geographic region appears to have significantly different approach/departure roughness from the others.

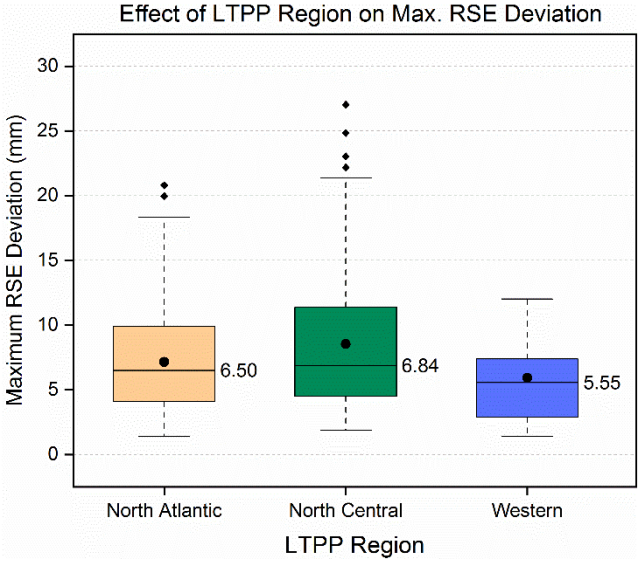

Source: FHWA.
1 mm = 0.039 inches.

A. Maximum RSE deviations.

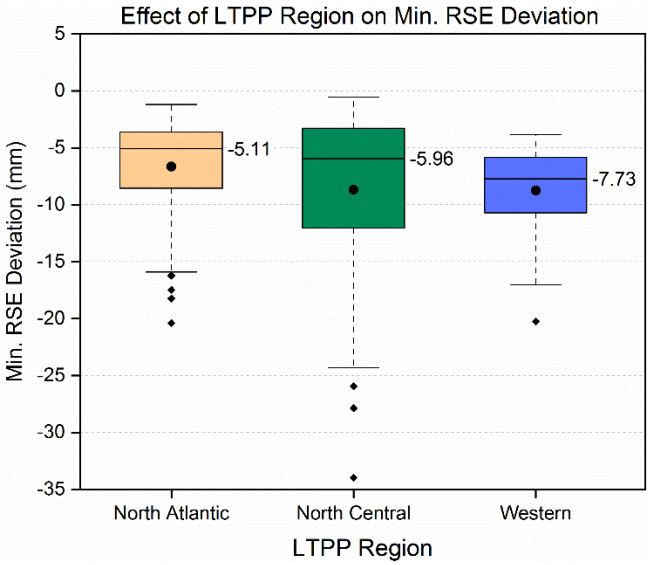

Source: FHWA.
1 mm = 0.039 inches.

B. Minimum RSE deviations.

Figure 22. Graphs. Maximum and minimum RSE deviations for approach and departure sections (combined) based on LTPP regions.

CHAPTER 3. ANALYSIS OF INERTIAL PROFILER DATA AND GROUPINGS

As previously mentioned, FHWA's Turner-Fairbank Highway Research Center evaluated inertial profiler datasets for 66 bridges across the United States. Because some profiles were collected in multiple lanes and directions of travel, these 66 bridges were presented in 112 profiles. The process and decisions made to obtain this number of profiles are discussed in the Description of Dataset Obtained from FHWA section in chapter 2. The characteristics (e.g., configuration, direction, number of passes, bridge length, age, ADT) for all bridges analyzed are in appendix A.

In addition to the differentiation applied to the approach, bridge, and departure sections of the profile data, a differentiation was made for each profile by the location along the profile. To ensure the profiling equipment has been calibrated and reached an adequate speed before recording information of the bridge profile, a distance of 275 m (902 ft) before the start sensor and 30 m (97 ft) after the end should be collected (Henderson et al. 2016). Because of the quantity of bridges in this study located on rural roads, there was no guarantee of the 275-m (902-ft) calibration distance before the structure. Therefore, the data included a distance of approximately 61 m (200 ft) on either side of the bridge deck, as was done in Henderson et al. (2016), to present only the portion of the bridge approach transition to be evaluated.

Separating the sections of each bridge profile differentiated bumps or rough sections specific to the approach and departure of the bridge. Roughness occurring on the deck of the bridge may be attributed to other causes not related to the purpose of this study. For this reason, roughness observed outside of the approach and departure sections established for each bridge was not considered in the statistical analysis of this project.

Each profile was analyzed using multiple filters to determine any trends from the data provided. The first filter applied was the Butterworth high-pass filter with a long wavelength cutoff of 91 m (298.5 ft). The Butterworth high-pass filter was applied to the raw data, and then analysis was performed using cross-correlation, IRI with 0.31-m (1-ft) segment length, RSE, and elevation versus distance. Although only the 0.31-m (1-ft) segment length was used for final statistical analyses, the 3.05- and 7.62-m (10- and 25-ft) segment lengths were still used as part of the analysis performed in ProVAL. Further information regarding these different analyses is provided in the following sections.

All data reduction on the raw data files was performed using ProVAL, a standardized software program for viewing and analyzing pavement profiles in a variety of ways. This program was developed with the support of FHWA and others as a primary tool to perform pavement profile analysis in a consistent manner across multiple transportation agencies. Aside from the cross-correlation, IRI, RSE, and elevation analyses used for this research, ProVAL can perform profile editing, power spectral density, profilograph simulation, and other analyses. Further information can be found on the software developer's website (The Transtec Group 2015).

CROSS-CORRELATION ANALYSIS

For each profile analyzed, between one and five passes by the profiler along the same segment were recorded. The repeatability of the data between successive passes can be assessed through cross-correlation analysis. The purpose of the cross-correlation analysis is to ensure the instrumentation being used is performing accurately. According to Perera and Kohn (2005, p. 28), there are three different ratings representing the agreement between profile measurements: "*repeatability* when it is applied to two measurements of the same profile by the same device, *reproducibility* when it is applied to two measurements of the same profile by different devices, and *accuracy* when a measurement from one of the devices is deemed to be correct." Because the same profiling equipment was used for all passes on a single bridge, the cross-correlation analysis in this study provided a repeatability rating. Although using the same profiler provides greater consistency between passes, any variation in a later position within the lane or longitudinal position for the start and end of the bridge deck can cause error in the cross-correlation rating.

It is important to note that cross-correlation analysis can be performed only when data along the same segment are collected by multiple passes of the profiler; it is impossible to comment on the accuracy of the data collected for bridge approach locations where data were recorded from only one pass. This was the case for 31 of the 112 profiles analyzed in this research effort. Analysis of the data required the assumption that the profile data provided from the one pass were accurate.

The cross-correlation between data from multiple passes can be calculated using different approaches. The method used in ProVAL produces an output in the form of percentage. This calculation is performed based on the equation in figure 23 (Karamihas and Gillespie 2002; Wang and Glintsch 2010):

$$R_{pq}(\delta) = \frac{100}{\sigma_p \sigma_q} \sum_{i=1}^{N} P_i Q_{i+\frac{\delta}{\Delta}}$$

Figure 23. Equation. Cross-correlation rating formula (Wang and Glintsch 2010).

Where:

$R_{pq}(\delta)$ = cross-correlation rating.
P_i = profile measurement P at i sampling number.
Q_i = profile measurement Q at i sampling number.
δ = offset distance between two profile measurements.
Δ = sampling interval.
σ_p = standard deviation of P.
σ_q = standard deviation of Q.

The equation in figure 23 results in cross-correlation ratings from 0 to 100 percent, where the greater the rating, the more similarities between passes. According to the American Association of State Highway and Transportation Officials R56 standard, a rating of 92 percent is preferred for profiler repeatability (AASHTO 2018). Note that an alternative form of the equation that does not include the 100 in the coefficient fraction can be used. In this case, the cross-correlation rating will be from 0 to 1.

Using the Automated Profile Synchronization tool in ProVAL, the correlations of all passes for each bridge were measured. These correlations used the center profile of each pass for the approach, bridge, and departure sections. For 81 bridge profiles that included multiple passes (out of 112 total bridge profiles), the first recorded pass was used as the basis to compare the additional passes. A sample of the maximum correlation values collected is presented in table 2, and the entire collection of data is included in appendix B. The contents of table 2 were selected to show cross-correlation values for the possible combinations of bridge configuration, direction of data collection, and location (e.g., approach, bridge, and departure sections). Results are presented as a single value for bridges with only two passes, as a range of values for bridges with at least three passes, and as not applicable (N/A) for bridges with only a single pass.

Table 2. Cross-correlation values and ranges in percent.

State	Test ID	Configuration	Direction	Approach	Bridge	Departure
DE	1	Perp_GRS	East	97.33	96.37	96.70
			West	97.92	98.37	99.45
MD	1	Skew_GRS	East	92.81	94.65	98.87
			West	89.90*–95.56	90.19*–92.89	87.12*–94.79
MI	1	Perp_GRS	N/A	99.21	99.23	99.45
NY	104	Perp_Conv	N/A	93.06–96.78	94.84–97.32	97.96–99.44
OH	27	Skew_GRS	East	92.73	92.74	91.25*
			West	97.55	99.44	97.55
SD	101	Skew_Conv	East	N/A	N/A	N/A
			West	99.75	98.79	95.56

*Value outside the 92-percent tolerable range.

A minimum of three passes over a bridge should be collected to ensure reliable data readings that can be verified with the cross-correlation method. Additional standards, used by most State agencies, require at least two profile readings taken along each wheel path (Henderson et al. 2016). The data provided for the 66 bridges in this analysis included each wheel path and an additional profile along the center of the lane; the number of passes ranged from one to five passes per direction. Standards also suggest these measurements be taken in both directions along each bridge; however, this was not a reality with the data available. Although measurements taken in both directions provide a more complete depiction of each bridge, the profiles in each direction were treated as unique individual structures for the purpose of this study (i.e., if profile data were collected for both travel directions of a particular bridge, those datasets were treated as belonging to separate structures). This approach was justified because for several of the bridges, the two travel directions were not connected at the median.

BRIDGE ABUTMENT TYPE

The first variable (i.e., category) analyzed with the profiler data was the bridge abutment type (conventional versus GRS). The use of GRS for bridge supports began in the 1970s by the U.S. Forest Service for logging roads (Adams et al. 2011). Since then, the design has gained popularity in various transportation agencies for several reasons, one being alleviation of the BEB phenomenon (Lee and Wu 2004; Adams et al. 2007; Nicks and Adams 2017). The impact of the abutment type was therefore quantified to determine whether a GRS design results in improvement of the roughness of bridge profiles.

The first comparative analysis, shown in figure 24, displays the maximum IRI values for the 0.31-m (1-ft) segment length based on bridge abutment type. There was variability in the median values between the GRS and conventional abutment types. The GRS abutment had a slightly lower median value; however, the maximum value was higher than that of the conventional abutment type. Additionally, the GRS abutment type had more outliers. The quantity of outliers may be related to the number of bridges within the dataset corresponding to the GRS category. There were more GRS (76.8 percent) than conventional bridges (23.2 percent) in the analysis.

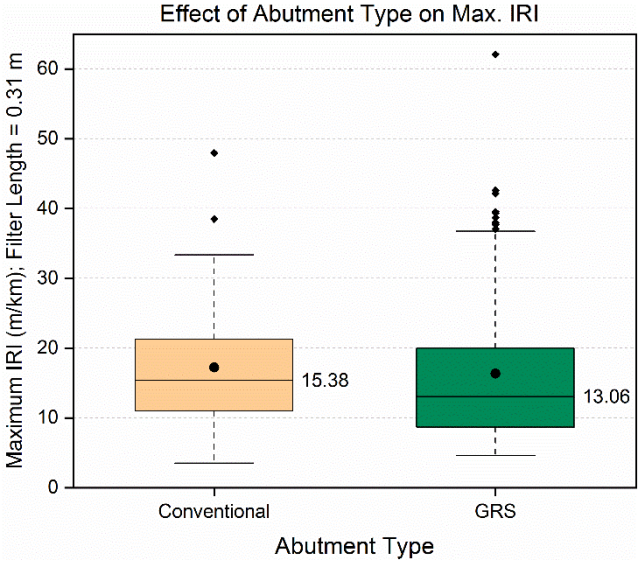

Source: FHWA.
1 m = 3.28 ft; 1 m/km = 5.28 ft/mi.

Figure 24. Graph. Maximum IRI values for 0.31-m (1-ft) segment length for approach and departure sections (combined) based on abutment type.

Among the bridge profiles analyzed under the current study, bridges with GRS abutments had more variability in approach/departure roughness compared to bridges with conventional abutments. While the difference in values was not statistically significant, it was noteworthy.

The dataset did not include a sufficient number of bridges in each category in individual States to facilitate a State-by-State performance comparison of approach/departure roughness between different bridge types. New York had data from 11 GRS and 5 conventional abutment bridges. Figure 25 compares the maximum IRI values for New York bridges. GRS bridges in New York showed significantly lower approach/departure roughness compared to conventional bridges.

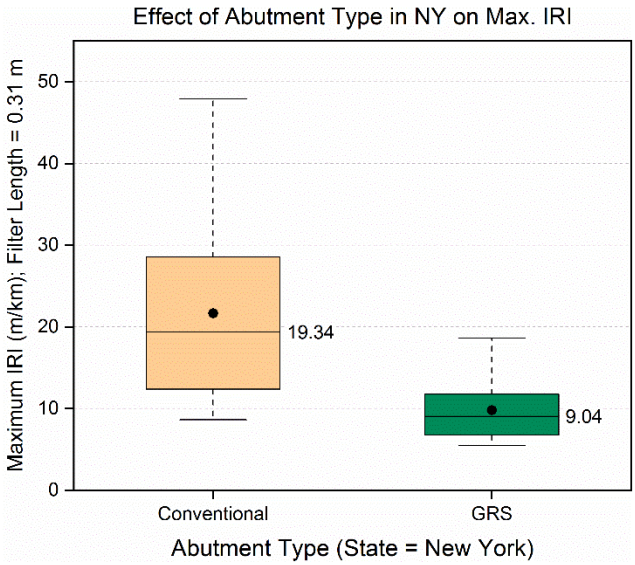

Source: FHWA.
1 m = 3.28 ft; 1 m/km = 5.28 ft/mi.

Figure 25. Graph. Maximum IRI values for 0.31-m (1-ft) segment length for approach and departure sections (combined) based on abutment type in New York.

Trends similar to those shown in figure 25 were seen for the maximum and minimum RSE values for bridges in New York (figure 26-A and figure 26-B). Irrespective of whether the maximum or minimum RSE deviation was used as the metric, the GRS bridges exhibited significantly smoother approach/departure profiles compared to conventional bridges. When interpreting RSE deviations, the maximum and minimum values indicated the deviation upward or downward from a flat, perfectly smooth surface (i.e., the bump and dip, respectively). The maximum RSE deviation values indicated upward deviations from a perfectly horizontal surface, whereas the minimum RSE deviation values indicated downward deviations from a horizontal surface. Therefore, RSE deviations, minimum or maximum, closest to 0 mm represented a smoother profile. Another approach to analyze RSE data was comparing the total RSE deviations (calculated as the sum of absolute values of maximum and minimum RSE deviations) for each profile measurement. However, this approach was not adopted in the current study.

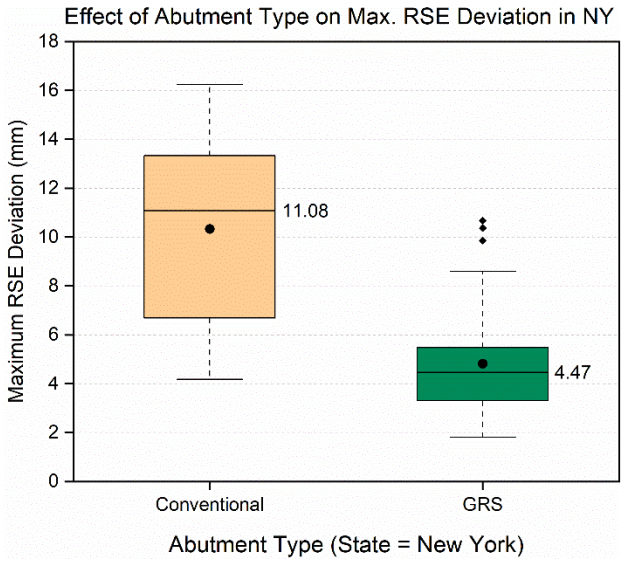

Source: FHWA.
1 mm = 0.039 inch.

A. Maximum RSE deviations.

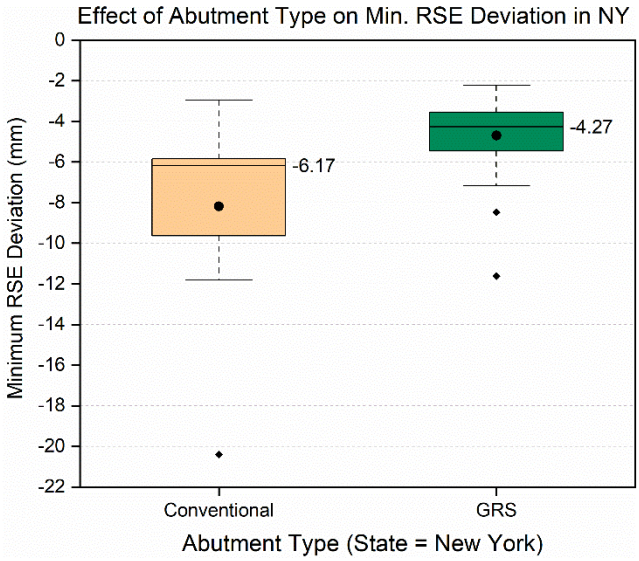

Source: FHWA.
1 mm = 0.039 inch.

B. Minimum RSE deviations.

Figure 26. Graphs. Maximum and minimum RSE deviations for approach and departure sections (combined) based on abutment type in New York.

Figure 27 presents the maximum and minimum RSE deviations of the bridge profiles based on abutment type. Considering the maximum and minimum RSE deviations together, there was minimal variation in the full range between the GRS and conventional abutment types. The maximum RSE deviations shown in figure 27-A had similar values for both abutment types with a slightly higher median value for the conventional abutment. Values shown in figure 27-B also had comparable values between both abutment types; however, the median value for the

conventional abutment was further from the 0 value than for the GRS abutment. Considering figure 27-A and figure 27-B together, the combined range for absolute minimum and absolute maximum values was similar for both abutment types with a greater frequency of outliers for the GRS abutment type.

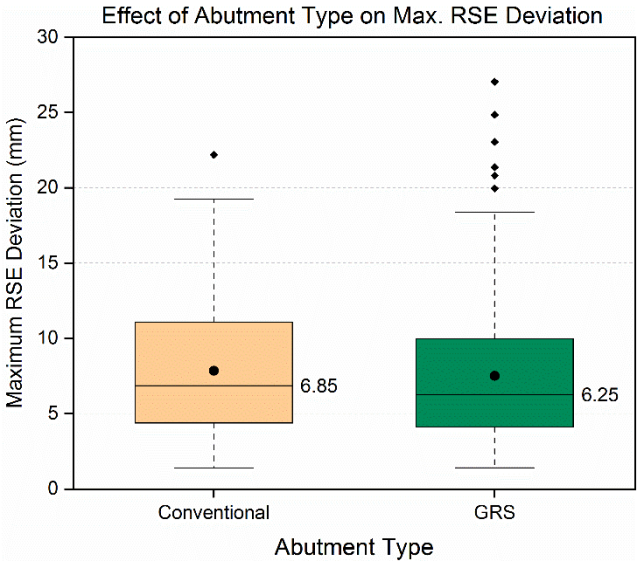

Source: FHWA.
1 mm = 0.039 inch.

A. Maximum RSE deviations.

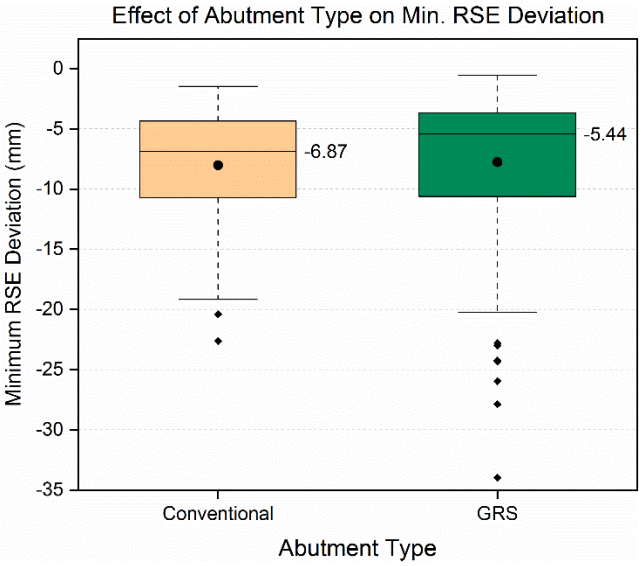

Source: FHWA.
1 mm = 0.039 inch.

B. Minimum RSE deviations.

Figure 27. Graphs. Maximum and minimum RSE deviations for approach and departure sections (combined) based on abutment type.

BRIDGE CONFIGURATION

An additional comparative analysis was performed by ignoring the abutment type for each bridge and only comparing those with perpendicular versus skewed abutment configurations. The skew angle was collected based on the information provided in LTBP InfoBridge; however, the magnitude of the skew angle was not included in this analysis (FHWA 2019). Bridges with skew angles greater or less than 0 degrees were categorized as skewed whereas those with skew angles of 0 degrees were categorized as perpendicular. Figure 28 compares the maximum IRI values for bridges with perpendicular versus skewed abutments.

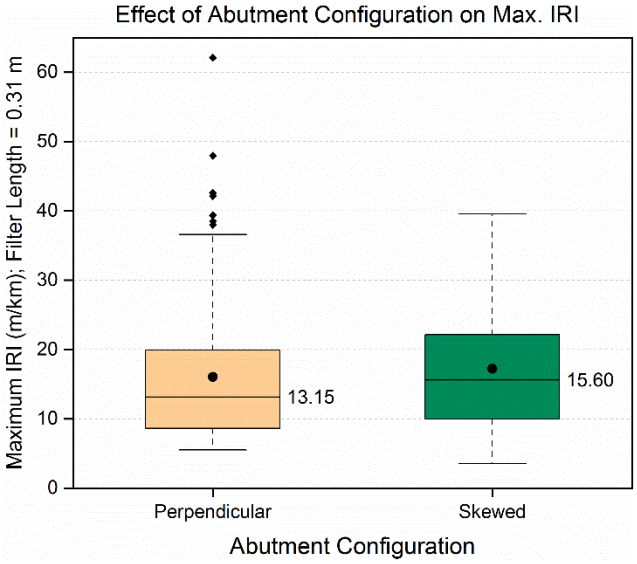

Source: FHWA.
1 m = 3.28 ft; 1 m/km = 5.28 ft/mi.

Figure 28. Graph. Maximum IRI values for 0.31-m (1-ft) segment length for approach and departure sections (combined) based on bridge configuration.

When analyzing the data presented in figure 28, the median value of maximum IRI was higher for skewed than it was for perpendicular bridges. However, the perpendicular bridges contain outliers upward of 60 m/km (316.8 ft/mi). A similar comparison was performed for perpendicular- versus skewed-abutment bridges in Ohio (figure 29). Data from Ohio consisted of 13 skewed- and 14 perpendicular-abutment bridges. The perpendicular bridge category in figure 29 showed slightly higher median value and a greater number of outlier data points with high maximum IRI values.

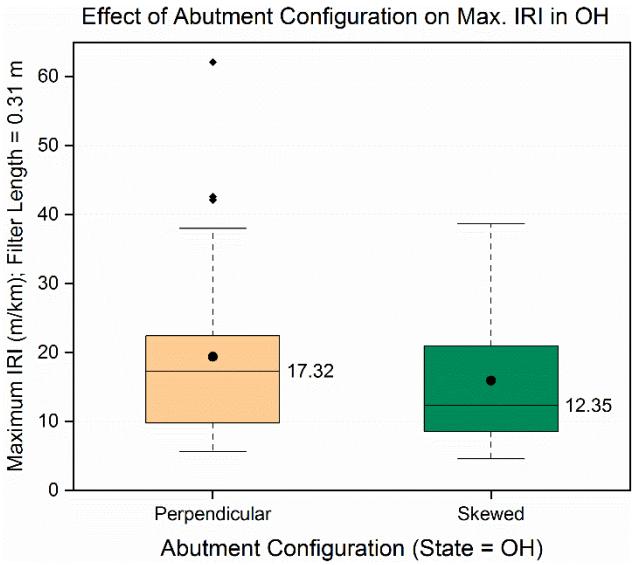

Source: FHWA.
1 m = 3.28 ft; 1 m/km = 5.28 ft/mi.

Figure 29. Graph. Maximum IRI values for 0.31-m (1-ft) segment length for approach and departure sections (combined) based on bridge configuration in Ohio.

Figure 30 compares the maximum and minimum RSE deviations for bridges based on their approach angle. Similar to the trends in figure 28, bridges with skewed approaches (figure 30-B) had median values further from 0, while those with perpendicular approaches (figure 30-A) had higher overall maximum values.

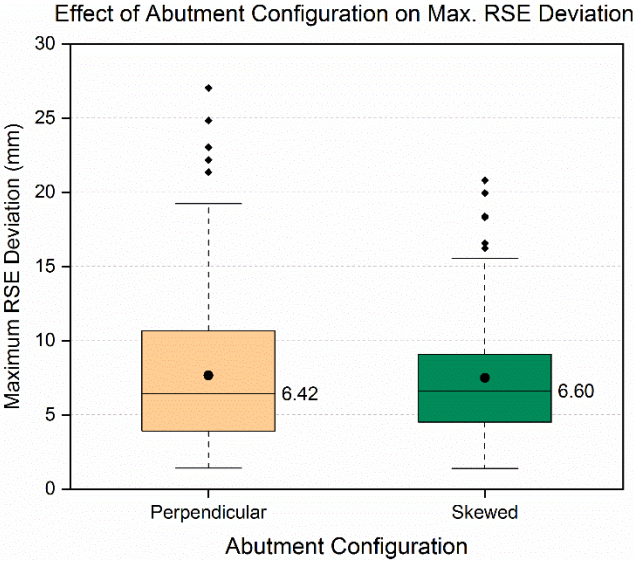

Source: FHWA.
1 mm = 0.039 inch.

A. Maximum RSE deviations.

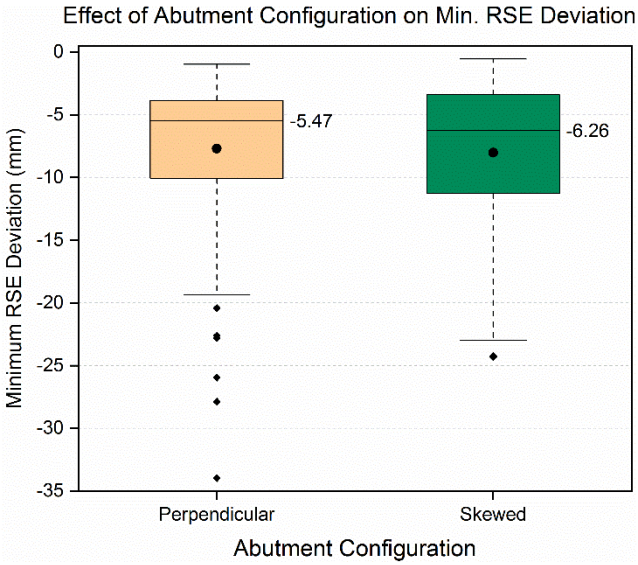

Source: FHWA.
1 mm = 0.039 inch.

B. Minimum RSE deviations.

Figure 30. Graphs. Maximum and minimum RSE deviations for approach and departure sections (combined) based on bridge configuration.

BRIDGE CATEGORIES FROM GEOMETRY

The original list of bridges grouped bridges based on the following abutment type (i.e., GRS or conventional) and configuration (i.e., perpendicular or skewed):

- Perp_Conv (8 bridges).
- Perp_GRS (30 bridges).
- Skew_Conv (7 bridges).
- Skew_GRS (21 bridges).

The first comparative analysis, shown in figure 31, shows the maximum IRI values for the 0.31-m (1-ft) segment length based on category. When comparing conventional abutments, the skewed approach had a higher median value but the perpendicular approach had a higher maximum value. When comparing GRS abutments, those where the abutment was perpendicular to the travel direction resulted in relatively lower median IRI values (12.75 m/km (7.9 m/hr)) compared to those with skewed abutments (14.91 m/km (9.2 m/hr)).

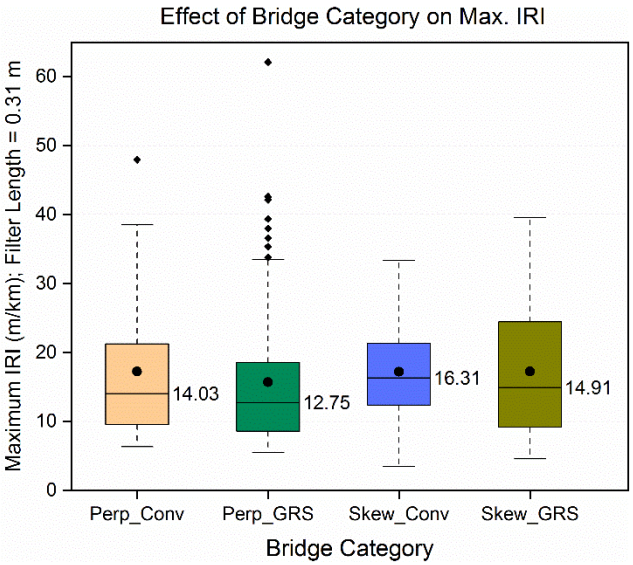

Source: FHWA.
1 m = 3.28 ft; 1 m/km = 5.28 ft/mi.

Figure 31. Graph. Maximum IRI values for 0.31-m (1-ft) segment length for approach and departure sections (combined) based on bridge category.

Only bridges with perpendicular approaches had outlying values, the highest of which was for GRS abutments. The higher outlier for the Perp_GRS category was likely due to the larger dataset used in the analysis as compared to that of the Perp_Conv category. The median values show minimal variation from one bridge category to another, indicating the absence of statistically significant differences within the limited dataset.

The four categories were also compared based on maximum and minimum RSE deviations, as shown in figure 32. Compared to the plots shown in figure 31, there was less consistency with the RSE deviations based on each category. When considering the maximum IRI values, the Skew_GRS category displayed the largest interquartile range, as shown in figure 31; however, the results of the maximum and minimum RSE deviations present different results. If considering only the maximum RSE deviations, as shown in figure 32-A, the Perp_Conv category had the largest median IRI and IQR values, while the Skew_Conv category showed the smallest IQR. When considering the minimum RSE deviations, as shown in figure 32-B, the largest interquartile range and deviation value occurred in the Skew_GRS category. However, based on the range of data distribution, this difference was not statistically significant.

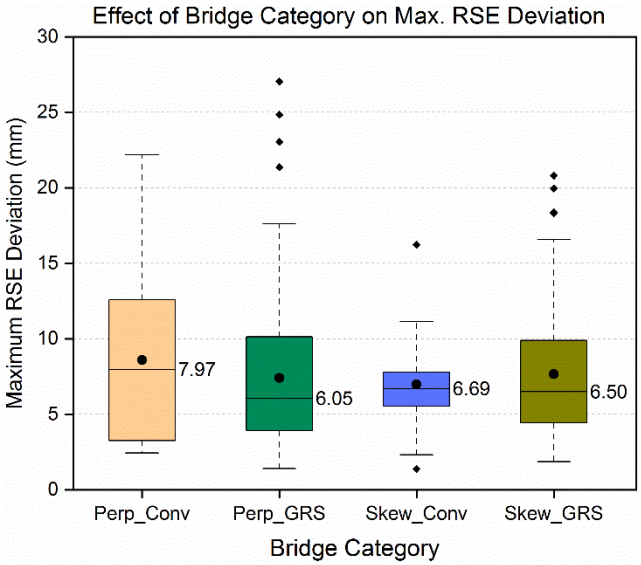

Source: FHWA.
1 mm = 0.039 inch.

A. Maximum RSE deviations.

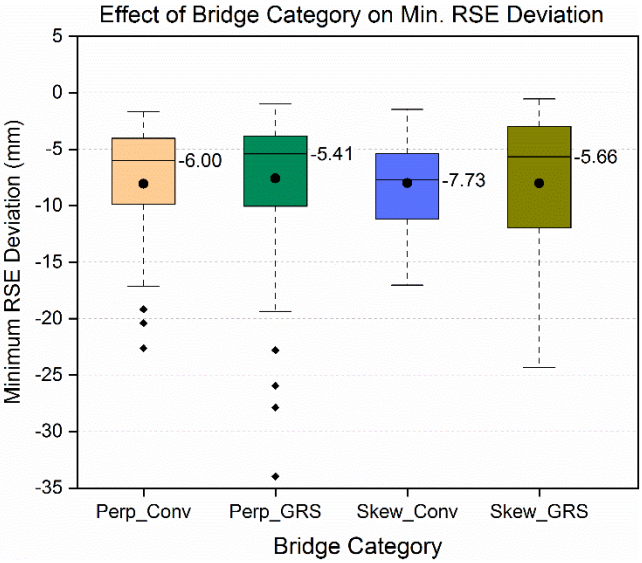

Source: FHWA
1 mm = 0.039 inch.

B. Minimum RSE deviations.

Figure 32. Graphs. Maximum and minimum RSE deviations for approach and departure sections (combined) based on bridge category.

BRIDGE LENGTH

The collected data were further analyzed based on categories of information collected from LTBP InfoBridge, the first of which was bridge length. Previously, the importance of bridge length was discussed in regard to the impact of segment lengths used for IRI calculations. Bridge length was particularly important for short-span bridges; however, further analysis assessed

whether or not bridge length had any correlation with approach/departure roughness. Based on the range of values collected for the bridges analyzed, different categories for bridge length were developed as follows:

- <15 m (<49.2 ft) (36 bridges).
- >15 m (>49.2 ft) (30 bridges).

Figure 33 shows maximum IRI values based on the categories for bridge length. Bridges with lengths greater than 15 m (49.2 ft) presented lower median IRI and IQR values. The research team was unable to identify any justification for this trend. Theoretically, bridge length should not impact approach/departure roughness, as approach design is independent of span length.

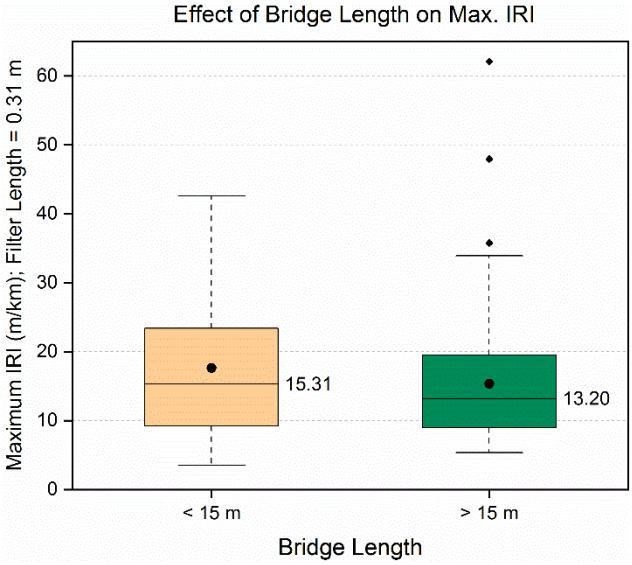

Source: FHWA.
1 m = 3.28 ft; 1 m/km = 5.28 ft/mi.

Figure 33. Graph. Maximum IRI values for 0.31-m (1-ft) segment length for approach and departure sections (combined) based on bridge length.

Figure 34-A and figure 34-B show the maximum and minimum RSE deviations, respectively, based on the categories for bridge length. The maximum and minimum RSE deviations were similar to those from the IRI analysis (figure 33); smaller median values were observed for bridges with lengths greater than 15 m (49.2 ft), although the difference was relatively small. The trends between the categories for bridge length were similar between the maximum and minimum plots in figure 34.

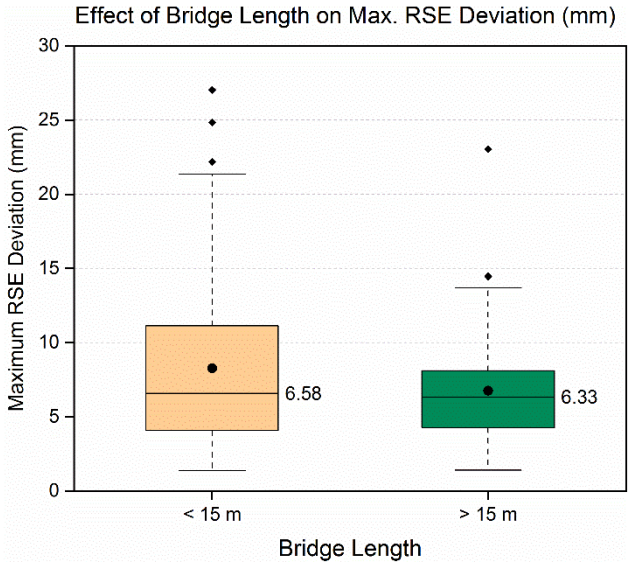

Source: FHWA.
1 m = 3.28 ft; 1 mm = 0.039 inch.

A. Maximum RSE deviations.

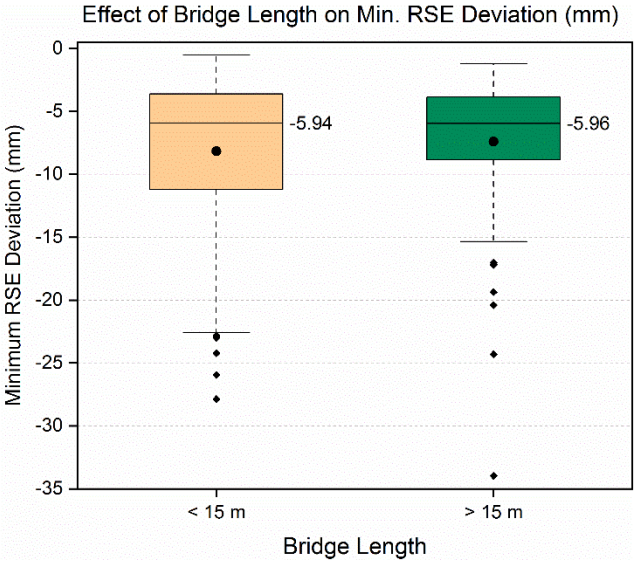

Source: FHWA.
1 mm = 0.039 inch.

B. Minimum RSE deviations.

Figure 34. Graphs. Maximum and minimum RSE deviations for approach and departure sections (combined) based on bridge length.

BRIDGE AGE

Another category evaluated from the LTBP InfoBridge database was the age of a bridge. The age of a bridge was determined based on the date of most recent construction and the date the profile was collected. Bridges were grouped into two categories based on their age as follows:

- <5 yr (30 bridges).
- >5 yr (28 bridges).

While 5 yr is a relatively short period to consider, this threshold was selected for an even distribution of bridges between the two categories. Since GRS bridges are relatively new and make up the majority of the data in this current project, the distribution of data was centered around a younger age. The categories were then compared for maximum IRI values (figure 35) and minimum and maximum RSE deviations (figure 36).

Figure 35 displays the maximum IRI values for the 0.31-m (1-ft) segment length for each category of bridge age. There was only slight variation in the median values for the two categories; there were more prominent differences in the IQR and whisker lengths. Older bridges corresponded to higher roughness values compared to younger bridges, which was similar to what is shown in figure 36 for the maximum and minimum RSE deviations. Many aspects of bridge-age analysis were uncertain based on the information available from LTBP InfoBridge. In addition, information about the dates of maintenance were unknown; therefore, there were potential inconsistencies in the performance of each structure when analyzed by age. Further research is required to differentiate the performance of structures that have undergone maintenance.

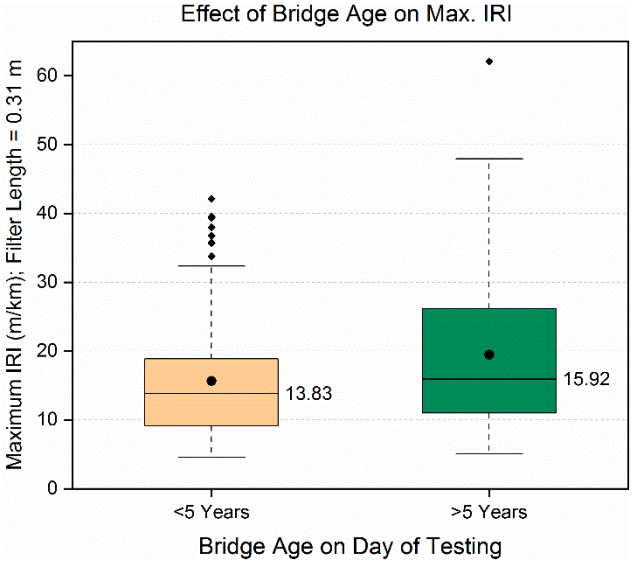

Source: FHWA.
1 m = 3.28 ft; 1 m/km = 5.28 ft/mi.

Figure 35. Graph. Maximum IRI values for 0.31-m (1-ft) segment length for approach and departure sections (combined) based on bridge age.

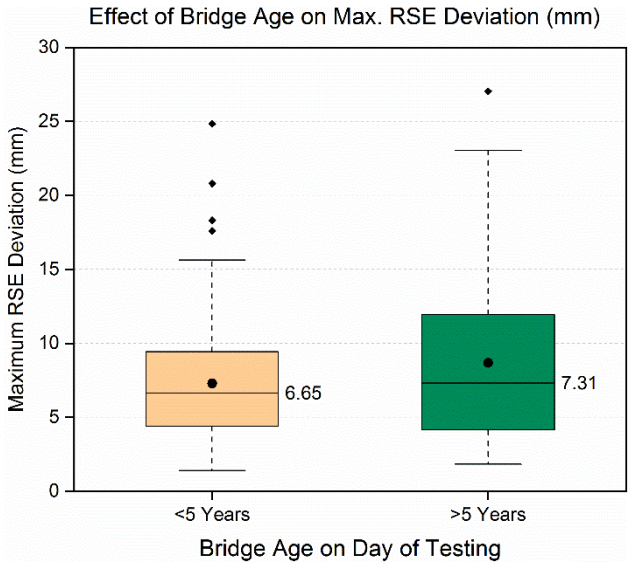

Source: FHWA.
1 mm = 0.039 inch.

A. Maximum RSE deviations.

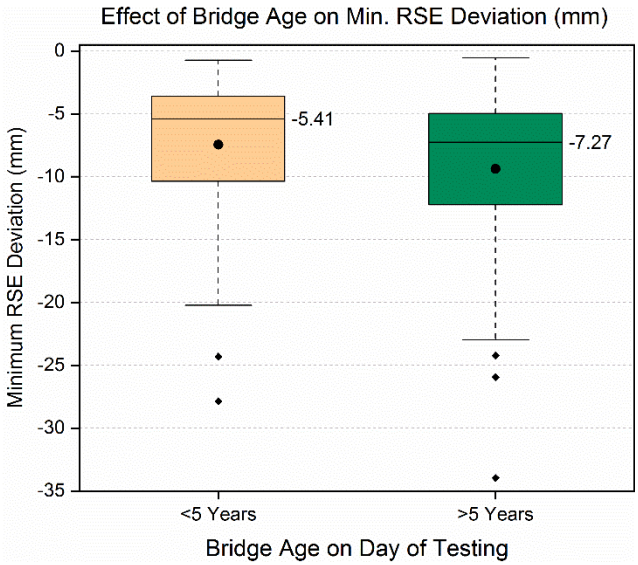

Source: FHWA.
1 mm = 0.039 inch.

B. Minimum RSE deviations.

Figure 36. Graphs. Maximum and minimum RSE deviations for approach and departure sections (combined) based on bridge age.

AVERAGE DAILY TRAFFIC

The next category evaluated for analysis was based on the ADT for each bridge. Based on the range of values extracted from LTBP InfoBridge, the following categories were defined:

- <300 ADT (25 bridges).
- >300 ADT (33 bridges).

ADT values correspond to the year during which profile data were collected. Approach/departure roughness values for the different ADT categories were compared based on the maximum IRI value and maximum and minimum RSE deviation values, as seen in figure 37 and figure 38, respectively.

Figure 37 shows a decrease in roughness in bridges with ADT greater than 300. There were a number of outliers in bridges with higher ADT levels even though all the box plot parameters (e.g., median IRI, IQR) for ADT greater than 300 were lower.

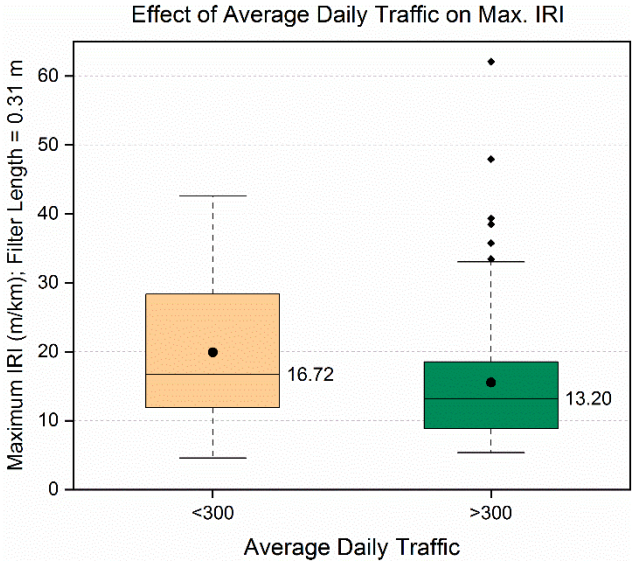

Source: FHWA.
1 m = 3.28 ft; 1 m/km = 5.28 ft/mi.

Figure 37. Graph. Maximum IRI values for 0.31-m (1-ft) segment length for approach and departure sections (combined) based on ADT.

Similar to the results in figure 37, the overall trend of minimum–maximum RSE ranges decreased as ADT values increased, as shown in figure 38. Figure 38-A and figure 38-B show similar trends to those for maximum IRI values. There were maximum RSE outliers for both ADT categories.

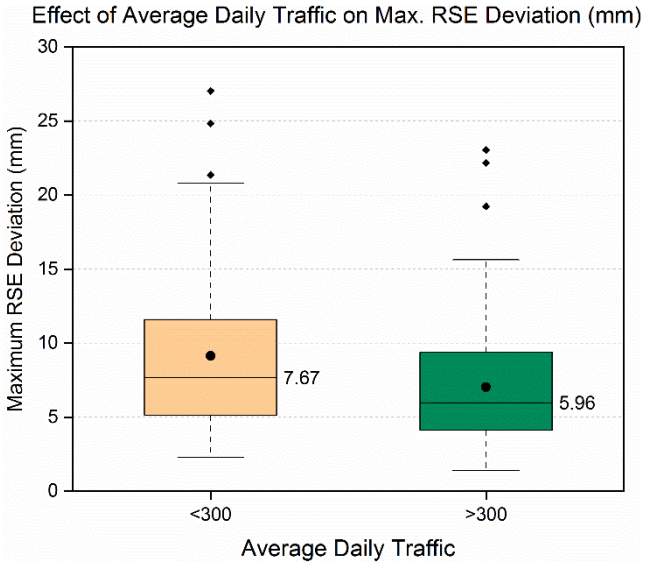

Source: FHWA.
1 mm = 0.039 inch.

A. Maximum RSE deviations.

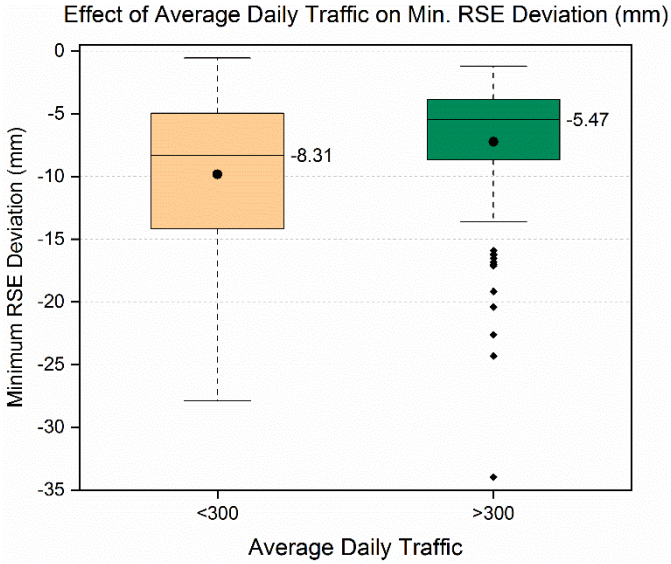

Source: FHWA.
1 mm = 0.039 inch.

B. Minimum RSE deviations.

Figure 38. Graphs. Maximum and minimum RSE deviations for approach and departure sections (combined) based on ADT.

While ADT was a key component in assessing bridge approach rideability, there are other considerations to understand in combination with ADT. A low ADT value indicates that a bridge is not commonly used, potentially requiring less maintenance, while a high ADT indicates more usage and thus potentially more required maintenance to ensure adequate serviceability of the bridge. No conclusion can be drawn regarding the effect of ADT on bridge approach/departure roughness without further information about maintenance frequency and history.

FREEZE/THAW CYCLES PER YEAR CORRELATED TO BRIDGE APPROACH/DEPARTURE ROUGHNESS

Further analysis based on factors potentially affecting bridge approach roughness included the number of freeze/thaw cycles per year to which a structure was exposed. The number of freeze/thaw cycles per year can have a large negative impact on pavement performance and impacts bridge contraction/expansion. The movement at the bridge approach interface against the backfill can lead to joint deterioration for conventional structures and cracked pavements causing water infiltration; these phenomena can potentially aggravate the BEB problem. Based on values found in LTBP InfoBridge, bridges were divided into the following categories based on freeze/thaw cycles per year:

- 50–75 cycles/yr (18 bridges).
- >75 cycles/yr (40 bridges).

The categories were then compared for approach/departure roughness based on the maximum IRI (figure 39) and maximum and minimum RSE deviation values (figure 40). The lowest IRI values were observed for bridges experiencing a lower number of freeze/thaw cycles per year (figure 39).

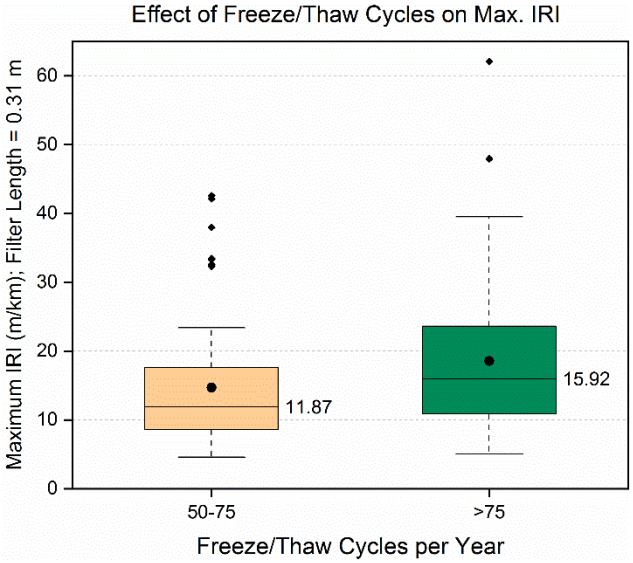

Source: FHWA.
1 m = 3.28 ft; 1 m/km = 5.28 ft/mi.

Figure 39. Graph. Maximum IRI values for 0.31-m (1-ft) segment length for approach and departure sections (combined) based on freeze/thaw cycles per year.

The maximum and minimum RSE deviations for the different freeze/thaw cycles per year categories are shown in figure 40. The different freeze/thaw cycle categories showed similar trends as those for the IRI maximum values, with higher values and ranges occurring in the higher freeze/thaw cycles per year category. The lower freeze/thaw cycles per year group showed two outlier points that were the highest in terms of maximum RSE deviation.

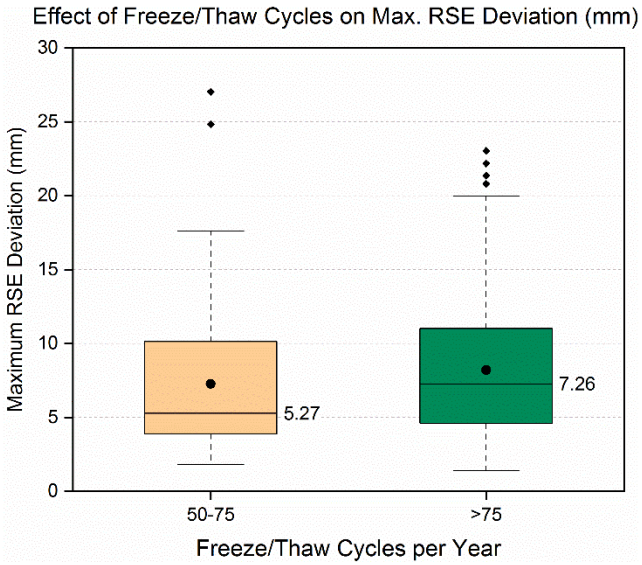

Source: FHWA.
1 mm = 0.039 inch.

A. Maximum RSE deviations.

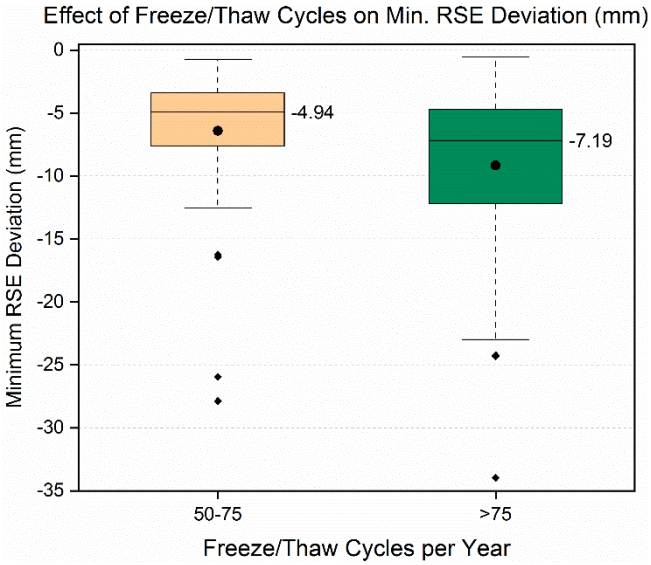

Source: FHWA.
1 mm = 0.039 inch.

B. Minimum RSE deviations.

Figure 40. Graphs. Maximum and minimum RSE deviations for approach and departure sections (combined) based on freeze/thaw cycles per year.

CHECKING THE STATISTICAL SIGNIFICANCE OF DIFFERENT FACTORS ON BRIDGE APPROACH/DEPARTURE ROUGHNESS

After comparing the data trends for different factors that can potentially affect bridge approach/departure roughness using boxplots, the next step involved conducing single-factor analysis of variance (ANOVA) tests to check the statistical significance of each factor (Ott and Longnecker 2015). In single-factor ANOVA tests, the null hypothesis (H_0) represents a case where the factor being considered does not have any significant effect on the dependent variable being analyzed. For example, when studying the effect of abutment configuration on IRI value, H_0 suggests that the mean IRI value is the same for bridges with perpendicular or skewed abutments. ANOVA calculations result in a *p*-value (i.e., statistical significance level). The *p*-value can be interpreted as the probability of observing results equal to, or more extreme than, those actually observed if the null hypothesis was true. In such a case, the H_0 was rejected if the *p*-value was smaller than the prespecified significance level (α), which was 0.05 in the current study; otherwise, H_0 could not be rejected (Heumann et al. 2016). Taking the example of effect of abutment configuration on IRI, if the resulting *p*-value was less than 0.05, the H_0 was rejected (i.e., abutment configuration had a significant effect on IRI). If the resulting *p*-value was greater than 0.05, the H_0 was not rejected, indicating the effect of abutment configuration on IRI was not significant.

The *p*-values corresponding to each of the factors considered in this study are listed in table 3. Whether data corresponded to an approach or departure segment did not have a statistically significant effect on roughness values. Taking examples of the IRI analysis, the *p*-value for the 0.31-m (1-ft) segment length was 0.383. Factors such as bridge age, traffic level, and number of freeze/thaw cycles per year had significant effects on the approach/departure roughness quantified using the maximum IRI with a segment length of 0.31 m (1 ft); the corresponding *p*-values were less than 0.05. Bridge length, age, traffic level, and LTPP region had significant effects on approach/departure roughness as defined by the maximum RSE deviations. The number of freeze/thaw cycles per year did not have a significant effect on maximum RSE deviation values. The factors that significantly affected minimum RSE deviation values were bridge age, traffic level, and number of freeze/thaw cycles per year. The factors significantly affecting bridge approach/departure roughness calculations vary from one quantification approach to another. The factors that significantly affected IRI, maximum RSE deviation, and minimum RSE deviation in the current dataset were not the same. Accordingly, the profile of a bridge approach may need to be analyzed using both IRI and RSE deviations, or a different index/indices not explored in this study, to identify factors that significantly affect the BEB. Further analysis of consistent and balanced datasets with equal representation of number of profiles with different factor combinations is required before these conclusions can be validated.

Table 3. Statistical significance levels for different factors affecting bridge approach/departure roughness.

Factor Being Analyzed	*p*-Value		
	Maximum IRI for 0.31-m (1-ft) Segment Length	Maximum RSE	Minimum RSE
Approach/departure	0.383	0.672	0.511
Bridge category	0.547	0.661	0.786
Bridge type	0.574	0.650	0.768
Abutment configuration	0.376	0.782	0.677
Bridge length (grouped)	0.098	0.016	0.316
Bridge age (grouped)	0.009	0.045	0.021
Traffic level (grouped)	0.003	0.002	0.002
Number of freeze/thaw cycles per year (grouped)	0.015	0.216	0.002
LTPP region	0.166	0.012	0.027

1 m = 3.28 ft.

CHAPTER 4. SUMMARY, CONCLUSIONS, AND FUTURE RESEARCH NEEDS

The primary objective of this study was to analyze inertial profiler data collected at 66 different bridge transitions from 14 different States and identify factors that affect the severity of the BEB. Significant findings, conclusions, and areas where future research efforts are needed to build on findings from this study are summarized as follows:

- The first task in the data analysis effort involved defining the approach and departure sections adjacent to a bridge structure, which was important to isolate the approach/departure roughness from the bridge deck roughness. Sectioning the bridges required some deviation from the practice of measuring 6 m (19.7 ft) before/after the interface between the approach roadway and the bridge deck, which was particularly relevant for short-span bridges. A modified method was used where 6-m (19.7-ft) segments were added before the start and after the end of the bridge deck; one-half of the bridge length was added to the deck side of each joint to mark the boundaries of the approach/departure sections for this analysis. As a result of the way approach/departure sections were defined, it is possible that bridge deck roughness could be included in the approach/departure definitions. In general, however, the approach/departure roughness values were greater than those on the bridge deck (figure 1).

- Data collected for different directions of travel were treated as if they belonged to two separate structures because several bridges with two directions of travel were not connected at the median.

- The IRI was the first method of quantifying bridge approach roughness in this study. A recommendation on the segment length used to calculate IRI at bridge approaches was not available, so three different segment lengths (0.31, 3.05, and 7.62 m [1, 10, and 25 ft]) were evaluated. From extensive analysis, the following was observed:

    - The standard segment length used for pavements (7.62 m [25 ft]) was too long to adequately capture the BEB magnitudes at bridge approaches. This became even more problematic for short-span bridges.

    - Although both 0.31- and 3.05-m (1- and 10-ft) segment lengths worked reasonably well, the research team used a segment length of 0.31 m (1 ft) to capture all necessary details related to approach/departure roughness.

    - Further validation through analyzing additional bridge approach/departure profile data is needed to use IRI to quantify bridge approach roughness.

    - Regardless of which segment length was used, any performance metric subsequently defined would be based on a singular segment length (i.e., if a segment length of 0.31 m [1 ft] was used analyze profile data, the performance metric would be based on the magnitude of those values). A different performance metric would be defined based on other segment lengths and the magnitude of those values.

- RSE deviation was selected as the second measure to quantify bridge approach/departure roughness. Data collected from the RSE analysis involved positive and negative values representing the deviation of the profile from a flat datum.

- Once the relevant IRI and RSE deviation values were calculated, the overall distributions of the datasets were investigated. Since the datasets were not normally distributed, researchers used a nonparametric descriptive statistics tool (i.e., box and whisker plots) to visualize and compare the datasets.

- Statistical analysis of the IRI and RSE deviation datasets revealed that there was no statistical difference between the BEB magnitudes at bridge approaches versus departures.

- Comparing the abutment types (i.e., GRS versus conventional) and abutment configurations (i.e., perpendicular versus skewed abutments) revealed no statistical significance when BEB magnitudes were considered. There were significantly higher numbers of GRS compared to conventional bridge abutments, which could impact findings. Future research should include an equal dataset and comparison of bridges with similar conditions to isolate the impact of bridge abutment type.

- Several of the States for which data were available contained data for one bridge type or the other. Data from New York included both GRS and conventional bridge types, and from those data, GRS bridges exhibited significantly lower IRI values compared to conventional bridges.

- This study attempted to identify other factors (e.g., bridge length, bridge age, ADT, number of freeze/thaw cycles per year) that can significantly affect the BEB. Although some factors (e.g., bridge age, ADT, number of freeze/thaw cycles per year, and LTPP region) appeared to be more significant than the others, the nature of the dataset available (i.e., unbalanced representation of different values within a given factor) raises questions about the statistical significance of some findings.

To build upon this study, it is recommended that a conscious effort be made to collect profile data for bridge approaches for different types of bridges in similar geographic locations. Data should also be collected for similar bridge types exposed to different traffic levels, climatic factors, and so on. Analysis of such consistent datasets using the methodology developed in this study will lead to better quantification of the BEB at bridge approaches and identification of factors that significantly affect the BEB. There is also a need to analyze the surface profiles collected at bridge locations on a regular basis to monitor the development of the BEB over time and assess whether or not maintenance activities succeed in remedying the problem. Once a sufficient number of profile measurements have been taken, performance metrics can be defined and used to monitor and evaluate the performance of bridge approaches using inertial profiler data.

APPENDIX A. BRIDGE CHARACTERISTICS

Appendix A outlines the bridge characteristics for all the collected profiles, including State, test ID, configuration, direction of travel, number of passes, bridge length, bridge age, ADT, number of freeze/thaw cycles per year, and the applicable LTPP region (table 4). The profiles collected in Utah were unique in that multiple lanes were tested in different directions rather than a single lane; bridge characteristics for the Utah bridge approaches are shown in table 5.

Table 4. Characteristics for all bridges.

State	Test ID	Configuration	Direction	Number of Passes	Length of Bridge (m)	Age at Test Date (yr)	ADT	Freeze/ Thaw Cycles/ Year	LTPP Region
CO	2	Skew_Conv	North	5	29.96	2	1,800	83	Western
			South	1					
DE	1	Perp_GRS	East	2	11.31	2	2,023	66	North Atlantic
			West	2					
DE	101	Skew_Conv	N/A	2	N/A	N/A	N/A	N/A	North Atlantic
MA	1	Skew_GRS	N/A	1	33.71	1	400	75	North Atlantic
MA	3	Perp_GRS	East	1	12.50	1	1,000	64	North Atlantic
			West	3					
MD	1	Skew_GRS	East	2	9.91	1	263	80	North Atlantic
			West	3					
MI	1	Perp_GRS	N/A	2	15.21	1	971	77	North Central
MT	1	Perp_GRS	North	5	11.80	2	470	118	Western
			South	1					
MT	2	Perp_Conv	N/A	1	29.69	9	470	118	Western
NY	1	Skew_GRS	N/A	5	30.21	0	702	73	North Atlantic
NY	2	Skew_GRS	East	4	19.51	3	900	91	North Atlantic
			West	2					
NY	3	Perp_GRS	North	3	20.39	3	1,340	91	North Atlantic
			South	2					
NY	4	Perp_GRS	East	2	13.41	4	1,100	96	North Atlantic
			West	5					

State	Test ID	Configuration	Direction	Number of Passes	Length of Bridge (m)	Age at Test Date (yr)	ADT	Freeze/ Thaw Cycles/ Year	LTPP Region
NY	5	Perp_GRS	North	1	18.81	1	280	96	North Atlantic
			South	3					
NY	6	Perp_GRS	North	2	13.99	2	282	68	North Atlantic
			South	2					
NY	7	Perp_GRS	East	2	17.10	5	966	73	North Atlantic
			West	2					
NY	8	Perp_GRS	North	1	23.20	4	671	73	North Atlantic
			South	2					
NY	9	Perp_GRS	North	1	14.30	5	635	73	North Atlantic
			South	2					
NY	11	Skew_GRS	North	3	28.71	4	628	73	North Atlantic
			South	1					
NY	12	Perp_GRS	N/A	2	16.49	4	3,118	73	North Atlantic
NY	101	Perp_Conv	N/A	4	24.41	11	670	96	North Atlantic
NY	102	Skew_Conv	North	2	64.31	50	310	96	North Atlantic
			South	4					
NY	103	Perp_Conv	N/A	3	21.31	6	310	96	North Atlantic
NY	104	Perp_Conv	N/A	3	47.91	15	937	73	North Atlantic
NY	105	Perp_Conv	N/A	1	9.39	69	257	68	North Atlantic
OH	2	Perp_GRS	N/A	2	8.20	7	100	75	North Central
OH	3	Perp_GRS	N/A	5	12.19	4	150	72	North Central
OH	5	Perp_GRS	N/A	1	7.59	8	143	72	North Central
OH	6	Skew_GRS	East	2	11.89	9	189	72	North Central
			West	2					
OH	7	Perp_GRS	N/A	2	17.71	5	175	75	North Central
OH	8	Perp_GRS	North	3	20.39	3	71	75	North Central
			South	1					
OH	9	Skew_GRS	N/A	2	8.11	6	111	75	North Central
OH	10	Perp_GRS	North	1	20.09	4	111	75	North Central
			South	2					

State	Test ID	Configuration	Direction	Number of Passes	Length of Bridge (m)	Age at Test Date (yr)	ADT	Freeze/ Thaw Cycles/ Year	LTPP Region
OH	11	Skew_GRS	North	1	16.49	9	125	75	North Central
			South	2					
OH	12	Perp_GRS	N/A	1	9.81	9	485	75	North Central
OH	13	Skew_GRS	East	3	7.89	8	46	75	North Central
			West	2					
OH	14	Skew_GRS	N/A	1	N/A	N/A	N/A	N/A	North Central
OH	15	Skew_GRS	North	1	12.50	5	89	75	North Central
			South	3					
OH	16	Skew_GRS	N/A	1	18.29	3	845	75	North Central
OH	17	Skew_GRS	N/A	1	7.32	5	152	75	North Central
OH	19	Skew_GRS	N/A	3	15.91	9	250	75	North Central
OH	20	Skew_GRS	North	2	N/A	N/A	N/A	N/A	North Central
			South	1					
OH	21	Skew_GRS	N/A	2	8.20	7	130	75	North Central
OH	22	Skew_GRS	East	2	N/A	N/A	N/A	N/A	North Central
			West	2					
OH	23	Perp_GRS	N/A	4	42.70	6	917	75	North Central
OH	24	Skew_GRS	East	2	24.99	10	135	78	North Central
			West	1					
OH	25	Perp_GRS	North	1	N/A	N/A	N/A	N/A	North Central
			South	3					
OH	26	Perp_GRS	North	2	N/A	N/A	N/A	N/A	North Central
			South	1					
OH	27	Skew_GRS	East	2	N/A	N/A	N/A	N/A	North Central
			West	2					
OH	29	Perp_GRS	North	1	11.31	3	200	75	North Central
			South	2					
OH	30	Skew_GRS	East	3	13.99	1	230	73	North Central
			West	1					
OH	103	Perp_Conv	East	1	N/A	N/A	N/A	N/A	North Central
			West	5					

State	Test ID	Configuration	Direction	Number of Passes	Length of Bridge (m)	Age at Test Date (yr)	ADT	Freeze/ Thaw Cycles/ Year	LTPP Region
PA	1	Perp_GRS	East	1	11.00	2	376	54	North Atlantic
			West	3					
PA	2	Perp_GRS	North	2	10.39	75	333	54	North Atlantic
			South	5					
PA	3	Skew_GRS	East	1	9.39	65	159	77	North Atlantic
			West	4					
PA	4	Skew_GRS	North	1	11.61	2	280	77	North Atlantic
			South	2					
PA	101	Skew_Conv	North	1	18.01	4	161	78	North Atlantic
			South	2					
SD	101	Skew_Conv	East	1	28.41	41	2,600	126	North Central
			West	2					
WA	1	Skew_GRS	North	3	12.19	2	169	99	Western
			South	2					
WA	2	Skew_Conv	North	4	27.40	7	368	99	Western
			South	1					
WI	1	Perp_GRS	North	2	12.19	3	1,200	74	North Central
			South	3					
WI	101	Perp_Conv	East	3	11.70	12	780	77	North Central
			West	1					
WV	1	Perp_GRS	East	1	14.30	2	9,000	77	North Atlantic
			West	3					
WV	101	Skew_Conv	North	1	18.99	2	450	77	North Atlantic
			South	2					

1 m = 3.28 ft.

Table 5. Characteristics for Utah bridges.

State	Test ID	Configuration	Direction	Lane	Number of Passes	Length of Bridge (m)	Age at Test Date (yr)	ADT	Freeze/ Thaw Cycles/ Year	LTPP Region
UT	1	Perp_GRS	N/A	Inside	3	18.01	2	4,051	136	Western
				Outside	2					
UT	2	Perp_Conv	East	Inside	4	34.50	42	6,657	136	Western
				Outside	2					
			West	Inside	3					
				Outside	3					

1 m = 3.28 ft.

APPENDIX B. CROSS-CORRELATION VALUES FOR PROFILE DATASETS

Appendix B provides all the cross-correlation values for the entire dataset analyzed in this study (table 6 and table 7).

Table 6. Cross-correlation values for profile datasets for all bridges.

State	Test ID	Configuration	Direction	Section	P01	P02	P03	P04	P05
CO	2	Skew_Conv	North	Approach	Base	99.66	95.65	98.74	98.74
				Departure	Base	98.74	99.67	97.81	98.40
			South	Approach	N/A	N/A	N/A	N/A	N/A
				Departure	N/A	N/A	N/A	N/A	N/A
DE	1	Perp_GRS	East	Approach	N/A	N/A	Base	97.33	N/A
				Departure	N/A	N/A	Base	96.70	N/A
			West	Approach	N/A	Base	97.92	N/A	N/A
				Departure	N/A	Base	99.45	N/A	N/A
DE	101	Skew_Conv	N/A	Approach	Base	98.82	N/A	N/A	N/A
				Departure	Base	93.33	N/A	N/A	N/A
MA	1	Skew_GRS	N/A	Approach	N/A	N/A	N/A	N/A	N/A
				Departure	N/A	N/A	N/A	N/A	N/A
MA	3	Perp_GRS	East	Approach	N/A	N/A	N/A	N/A	N/A
				Departure	N/A	N/A	N/A	N/A	N/A
			West	Approach	Base	98.75	99.71	N/A	N/A
				Departure	Base	93.11	99.05	N/A	N/A
MD	1	Skew_GRS	East	Approach	N/A	Base	92.81	N/A	N/A
				Departure	N/A	Base	98.87	N/A	N/A
			West	Approach	N/A	Base	95.56	89.80*	N/A
				Departure	N/A	Base	87.12*	94.79	N/A
MI	1	Perp_GRS	N/A	Approach	Base	99.21	N/A	N/A	N/A
				Departure	Base	99.45	N/A	N/A	N/A
MT	1	Perp_GRS	North	Approach	Base	80.56*	91.52*	97.72	95.20
				Departure	Base	97.69	99.03	99.71	97.24
			South	Approach	N/A	N/A	N/A	N/A	N/A
				Departure	N/A	N/A	N/A	N/A	N/A
MT	2	Perp_Conv	N/A	Approach	N/A	N/A	N/A	N/A	N/A
				Departure	N/A	N/A	N/A	N/A	N/A

State	Test ID	Configuration	Direction	Section	P01	P02	P03	P04	P05
NY	1	Skew_GRS	N/A	Approach	Base	99.21	93.10	99.18	93.16
				Departure	Base	98.79	85.92*	97.35	87.26*
NY	2	Skew_GRS	East	Approach	N/A	Base	99.46	99.18	99.33
				Departure	N/A	Base	93.87	99.49	98.61
			West	Approach	Base	N/A	93.21	N/A	N/A
				Departure	Base	N/A	95.60	N/A	N/A
NY	3	Perp_GRS	North	Approach	N/A	N/A	Base	87.97*	92.50
				Departure	N/A	N/A	Base	95.99	94.20
			South	Approach	Base	95.36	N/A	N/A	N/A
				Departure	Base	94.68	N/A	N/A	N/A
NY	4	Perp_GRS	East	Approach	Base	N/A	N/A	N/A	98.24
				Departure	Base	N/A	N/A	N/A	99.36
			West	Approach	Base	97.71	94.70	96.14	96.54
				Departure	Base	99.71	99.22	98.46	95.78
NY	5	Perp_GRS	North	Approach	N/A	N/A	N/A	N/A	N/A
				Departure	N/A	N/A	N/A	N/A	N/A
			South	Approach	Base	N/A	96.11	98.04	N/A
				Departure	Base	N/A	95.49	96.34	N/A
NY	6	Perp_GRS	North	Approach	Base	92.26	N/A	N/A	N/A
				Departure	Base	97.80	N/A	N/A	N/A
			South	Approach	N/A	N/A	Base	90.36*	N/A
				Departure	N/A	N/A	Base	94.27	N/A
NY	7	Perp_GRS	East	Approach	Base	98.57	N/A	N/A	N/A
				Departure	Base	97.27	N/A	N/A	N/A
			West	Approach	N/A	Base	98.44	N/A	N/A
				Departure	N/A	Base	90.97*	N/A	N/A
NY	8	Perp_GRS	North	Approach	N/A	N/A	N/A	N/A	N/A
				Departure	N/A	N/A	N/A	N/A	N/A
			South	Approach	Base	N/A	92.56	N/A	N/A
				Departure	Base	N/A	78.68*	N/A	N/A
NY	9	Perp_GRS	North	Approach	N/A	N/A	N/A	N/A	N/A
				Departure	N/A	N/A	N/A	N/A	N/A
			South	Approach	Base	98.14	N/A	N/A	N/A
				Departure	Base	91.18*	N/A	N/A	N/A

State	Test ID	Configuration	Direction	Section	P01	P02	P03	P04	P05
NY	11	Skew_GRS	North	Approach	Base	92.89	98.68	N/A	N/A
				Departure	Base	92.84	96.48	N/A	N/A
			South	Approach	N/A	N/A	N/A	N/A	N/A
				Departure	N/A	N/A	N/A	N/A	N/A
NY	12	Perp_GRS	N/A	Approach	N/A	Base	93.58	N/A	N/A
				Departure	N/A	Base	94.53	N/A	N/A
NY	101	Perp_Conv	N/A	Approach	N/A	Base	98.89	96.35	98.42
				Departure	N/A	Base	97.41	99.50	99.79
NY	102	Skew_Conv	North	Approach	N/A	N/A	N/A	Base	92.90
				Departure	N/A	N/A	N/A	Base	78.25*
			South	Approach	Base	90.86*	94.10	93.59	N/A
				Departure	Base	98.19	90.08*	90.08*	N/A
NY	103	Perp_Conv	N/A	Approach	N/A	N/A	Base	99.22	98.14
				Departure	N/A	N/A	Base	98.90	97.30
NY	104	Perp_Conv	N/A	Approach	Base	96.78	93.06	N/A	N/A
				Departure	Base	99.44	97.96	N/A	N/A
NY	105	Perp_Conv	N/A	Approach	N/A	N/A	N/A	N/A	N/A
				Departure	N/A	N/A	N/A	N/A	N/A
OH	2	Perp_GRS	N/A	Approach	Base	82.92*	N/A	N/A	N/A
				Departure	Base	90.68*	N/A	N/A	N/A
OH	3	Perp_GRS	N/A	Approach	Base	89.59*	96.99	97.67	96.54
				Departure	Base	91.83*	99.09	99.25	99.18
OH	5	Perp_GRS	N/A	Approach	N/A	N/A	N/A	N/A	N/A
				Departure	N/A	N/A	N/A	N/A	N/A
OH	6	Skew_GRS	East	Approach	N/A	Base	96.01	N/A	N/A
				Departure	N/A	Base	96.47	N/A	N/A
			West	Approach	Base	85.70*	N/A	N/A	N/A
				Departure	Base	84.75*	N/A	N/A	N/A
OH	7	Perp_GRS	N/A	Approach	Base	99.43	N/A	N/A	N/A
				Departure	Base	97.64	N/A	N/A	N/A
OH	8	Perp_GRS	North	Approach	Base	95.62	99.66	N/A	N/A
				Departure	Base	95.31	99.80	N/A	N/A
			South	Approach	N/A	N/A	N/A	N/A	N/A
				Departure	N/A	N/A	N/A	N/A	N/A

State	Test ID	Configuration	Direction	Section	P01	P02	P03	P04	P05
OH	9	Skew_GRS	N/A	Approach	N/A	Base	91.77*	N/A	N/A
				Departure	N/A	Base	99.57	N/A	N/A
OH	10	Perp_GRS	North	Approach	N/A	N/A	N/A	N/A	N/A
				Departure	N/A	N/A	N/A	N/A	N/A
			South	Approach	N/A	Base	88.75*	N/A	N/A
				Departure	N/A	Base	93.63	N/A	N/A
OH	11	Skew_GRS	North	Approach	N/A	N/A	N/A	N/A	N/A
				Departure	N/A	N/A	N/A	N/A	N/A
			South	Approach	Base	97.80	N/A	N/A	N/A
				Departure	Base	96.54	N/A	N/A	N/A
OH	12	Perp_GRS	N/A	Approach	N/A	N/A	N/A	N/A	N/A
				Departure	N/A	N/A	N/A	N/A	N/A
OH	13	Skew_GRS	East	Approach	Base	98.92	95.66	N/A	N/A
				Departure	Base	95.99	92.42	N/A	N/A
			West	Approach	Base	86.75*	N/A	N/A	N/A
				Departure	Base	95.16	N/A	N/A	N/A
OH	14	Skew_GRS	N/A	Approach	N/A	N/A	N/A	N/A	N/A
				Departure	N/A	N/A	N/A	N/A	N/A
OH	15	Skew_GRS	North	Approach	N/A	N/A	N/A	N/A	N/A
				Departure	N/A	N/A	N/A	N/A	N/A
			South	Approach	Base	98.56	99.55	N/A	N/A
				Departure	Base	93.10	98.37	N/A	N/A
OH	16	Skew_GRS	N/A	Approach	N/A	N/A	N/A	N/A	N/A
				Departure	N/A	N/A	N/A	N/A	N/A
OH	17	Skew_GRS	N/A	Approach	N/A	N/A	N/A	N/A	N/A
				Departure	N/A	N/A	N/A	N/A	N/A
OH	19	Skew_GRS	N/A	Approach	Base	95.22	82.82*	N/A	N/A
				Departure	Base	85.72*	89.32*	N/A	N/A
OH	20	Skew_GRS	North	Approach	Base	98.66	N/A	N/A	N/A
				Departure	Base	96.75	N/A	N/A	N/A
			South	Approach	N/A	N/A	N/A	N/A	N/A
				Departure	N/A	N/A	N/A	N/A	N/A
OH	21	Skew_GRS	N/A	Approach	N/A	Base	98.76	N/A	N/A
				Departure	N/A	Base	96.32	N/A	N/A

State	Test ID	Configuration	Direction	Section	P01	P02	P03	P04	P05
OH	22	Skew_GRS	East	Approach	Base	98.90	N/A	N/A	N/A
				Departure	Base	97.85	N/A	N/A	N/A
			West	Approach	Base	94.15	N/A	N/A	N/A
				Departure	Base	98.17	N/A	N/A	N/A
OH	23	Perp_GRS	N/A	Approach	Base	93.94	98.05	94.07	N/A
				Departure	Base	94.92	92.11	96.00	N/A
OH	24	Skew_GRS	East	Approach	Base	97.80	N/A	N/A	N/A
				Departure	Base	93.05	N/A	N/A	N/A
			West	Approach	N/A	N/A	N/A	N/A	N/A
				Departure	N/A	N/A	N/A	N/A	N/A
OH	25	Perp_GRS	North	Approach	N/A	N/A	N/A	N/A	N/A
				Departure	N/A	N/A	N/A	N/A	N/A
			South	Approach	Base	96.88	96.26	N/A	N/A
				Departure	Base	98.64	99.60	N/A	N/A
OH	26	Perp_GRS	North	Approach	Base	N/A	94.77	N/A	N/A
				Departure	Base	N/A	81.30*	N/A	N/A
			South	Approach	N/A	N/A	N/A	N/A	N/A
				Departure	N/A	N/A	N/A	N/A	N/A
OH	27	Skew_GRS	East	Approach	N/A	Base	92.73	N/A	N/A
				Departure	N/A	Base	91.25*	N/A	N/A
			West	Approach	Base	97.55	N/A	N/A	N/A
				Departure	Base	97.55	N/A	N/A	N/A
OH	29	Perp_GRS	North	Approach	N/A	N/A	N/A	N/A	N/A
				Departure	N/A	N/A	N/A	N/A	N/A
			South	Approach	N/A	Base	94.10	N/A	N/A
				Departure	N/A	Base	96.94	N/A	N/A
OH	30	Skew_GRS	East	Approach	Base	97.01	87.93*	N/A	N/A
				Departure	Base	96.17	98.59	N/A	N/A
			West	Approach	N/A	N/A	N/A	N/A	N/A
				Departure	N/A	N/A	N/A	N/A	N/A
OH	103	Perp_Conv	East	Approach	N/A	N/A	N/A	N/A	N/A
				Departure	N/A	N/A	N/A	N/A	N/A
			West	Approach	Base	97.04	87.26*	99.10	92.79
				Departure	Base	99.58	99.29	99.84	98.92

State	Test ID	Configuration	Direction	Section	P01	P02	P03	P04	P05
PA	1	Perp_GRS	East	Approach	N/A	N/A	N/A	N/A	N/A
				Departure	N/A	N/A	N/A	N/A	N/A
			West	Approach	Base	91.97*	85.25*	N/A	N/A
				Departure	Base	92.71	90.16*	N/A	N/A
PA	2	Perp_GRS	North	Approach	Base	N/A	92.50	N/A	N/A
				Departure	Base	N/A	98.37	N/A	N/A
			South	Approach	Base	98.57	96.70	98.94	97.41
				Departure	Base	98.07	98.51	98.26	98.68
PA	3	Skew_GRS	East	Approach	N/A	N/A	N/A	N/A	N/A
				Departure	N/A	N/A	N/A	N/A	N/A
			West	Approach	Base	76.59*	77.06*	91.83*	N/A
				Departure	Base	94.19	93.58	97.16	N/A
PA	4	Skew_GRS	North	Approach	N/A	N/A	N/A	N/A	N/A
				Departure	N/A	N/A	N/A	N/A	N/A
			South	Approach	N/A	Base	96.97	N/A	N/A
				Departure	N/A	Base	99.12	N/A	N/A
PA	101	Skew_Conv	North	Approach	N/A	N/A	N/A	N/A	N/A
				Departure	N/A	N/A	N/A	N/A	N/A
			South	Approach	Base	N/A	94.42	N/A	N/A
				Departure	Base	N/A	97.75	N/A	N/A
SD	101	Skew_Conv	East	Approach	N/A	N/A	N/A	N/A	N/A
				Departure	N/A	N/A	N/A	N/A	N/A
			West	Approach	Base	99.75	N/A	N/A	N/A
				Departure	Base	95.56	N/A	N/A	N/A
WA	1	Skew_GRS	North	Approach	N/A	Base	97.59	98.20	N/A
				Departure	N/A	Base	97.31	96.25	N/A
			South	Approach	N/A	Base	99.75	N/A	N/A
				Departure	N/A	Base	99.27	N/A	N/A
WA	2	Skew_Conv	North	Approach	Base	N/A	94.22	93.93	96.74
				Departure	Base	N/A	89.56*	88.11*	94.10
			South	Approach	N/A	N/A	N/A	N/A	N/A
				Departure	N/A	N/A	N/A	N/A	N/A
WI	1	Perp_GRS	North	Approach	Base	98.17	N/A	N/A	N/A
				Departure	Base	95.58	N/A	N/A	N/A

State	Test ID	Configuration	Direction	Section	P01	P02	P03	P04	P05
			South	Approach	Base	99.01	99.62	N/A	N/A
				Departure	Base	99.00	99.35	N/A	N/A
WI	101	Perp_Conv	East	Approach	Base	88.61*	95.66	N/A	N/A
				Departure	Base	98.83	98.12	N/A	N/A
			West	Approach	N/A	N/A	N/A	N/A	N/A
				Departure	N/A	N/A	N/A	N/A	N/A
WV	1	Perp_GRS	East	Approach	N/A	N/A	N/A	N/A	N/A
				Departure	N/A	N/A	N/A	N/A	N/A
			West	Approach	Base	97.57	97.00	N/A	N/A
				Departure	Base	98.84	97.51	N/A	N/A
WV	101	Skew_Conv	North	Approach	N/A	N/A	N/A	N/A	N/A
				Departure	N/A	N/A	N/A	N/A	N/A
			South	Approach	Base	N/A	96.44	N/A	N/A
				Departure	Base	N/A	98.14	N/A	N/A

*Values out of tolerance.

Table 7. Cross-correlation values for profile datasets for Utah bridges.

State	Test ID	Configuration	Direction	Lane	Section	P01	P02	P03	P04	P05
UT	1	Perp_GRS	N/A	Inside	Approach	Base	N/A	98.96	N/A	98.66
					Departure	Base	N/A	84.39*	N/A	87.87*
				Outside	Approach	Base	N/A	N/A	90.89*	N/A
					Departure	Base	N/A	N/A	98.87	N/A
UT	2	Perp_Conv	East	Inside	Approach	Base	92.79	94.11	N/A	99.44
					Departure	Base	95.80	96.47	N/A	94.51
				Outside	Approach	Base	N/A	N/A	94.15	N/A
					Departure	Base	N/A	N/A	95.89	N/A
			West	Inside	Approach	Base	N/A	94.09	95.20	N/A
					Departure	Base	N/A	94.93	91.86*	N/A
				Outside	Approach	N/A	Base	97.99	N/A	93.98
					Departure	N/A	Base	96.63	N/A	96.35

*Values out of tolerance.

APPENDIX C. MAXIMUM IRI VALUES AND MAXIMUM AND MINIMUM RSE DEVIATIONS

Appendix C provides the maximum IRI values along with the maximum and minimum RSE values for each profile evaluated (table 8 and table 9).

Table 8. Maximum IRI values and maximum and minimum RSE deviations for all bridges.

State	Test ID	Configuration	Direction	Section	Maximum IRI (m/km)	Minimum RSE (mm)	Maximum RSE (mm)
CO	2	Skew_Conv	North	Approach	29.773	−17.024	11.070
				Departure	17.855	−11.074	7.274
			South	Approach	21.811	−11.243	7.385
				Departure	20.847	−8.251	6.387
DE	1	Perp_GRS	East	Approach	8.642	−3.852	2.672
				Departure	7.472	−3.691	2.247
			West	Approach	9.902	−5.700	3.226
				Departure	9.236	−4.291	3.895
DE	101	Skew_Conv	N/A	Approach	7.796	−3.336	2.314
				Departure	3.540	−1.482	1.387
MA	1	Skew_GRS	N/A	Approach	9.216	−1.202	4.414
				Departure	5.379	−2.259	4.398
MA	3	Perp_GRS	East	Approach	17.517	−8.318	9.976
				Departure	15.615	−2.688	7.907
			West	Approach	18.529	−4.923	11.653
				Departure	18.108	−4.874	10.705
MD	1	Skew_GRS	East	Approach	28.996	−18.236	18.322
				Departure	15.693	−11.272	11.011
			West	Approach	16.450	−9.700	10.053
				Departure	36.753	−17.480	20.808
MI	1	Perp_GRS	N/A	Approach	8.333	−3.767	4.371
				Departure	7.569	−3.506	3.684
MT	1	Perp_GRS	North	Approach	12.677	−9.361	4.864
				Departure	15.188	−10.719	5.176
			South	Approach	17.998	−13.609	9.143
				Departure	27.506	−16.832	9.155

State	Test ID	Configuration	Direction	Section	Maximum IRI (m/km)	Minimum RSE (mm)	Maximum RSE (mm)
MT	2	Perp_Conv	N/A	Approach	19.902	−8.306	12.019
				Departure	13.365	−5.445	7.917
NY	1	Skew_GRS	N/A	Approach	10.235	−2.957	7.305
				Departure	6.373	−2.231	4.108
NY	2	Skew_GRS	East	Approach	15.660	−3.977	8.596
				Departure	11.068	−6.392	7.387
			West	Approach	9.922	−3.646	5.650
				Departure	8.030	−2.812	4.601
NY	3	Perp_GRS	North	Approach	6.163	−3.768	4.583
				Departure	13.208	−3.642	6.904
			South	Approach	9.958	−6.511	4.738
				Departure	7.283	−2.396	4.498
NY	4	Perp_GRS	East	Approach	11.637	−6.916	3.301
				Departure	6.019	−3.626	2.372
			West	Approach	6.702	−4.276	2.660
				Departure	10.108	−6.012	4.475
NY	5	Perp_GRS	North	Approach	8.187	−5.434	3.192
				Departure	5.964	−3.662	3.999
			South	Approach	7.614	−3.866	2.504
				Departure	12.657	−6.099	5.132
NY	6	Perp_GRS	North	Approach	15.822	−11.617	4.720
				Departure	12.877	−5.181	6.543
			South	Approach	17.576	−6.760	10.676
				Departure	13.863	−8.474	2.281
NY	7	Perp_GRS	East	Approach	6.016	−3.876	1.824
				Departure	11.191	−5.263	2.822
			West	Approach	8.810	−4.507	1.872
				Departure	5.506	−3.360	2.586
NY	8	Perp_GRS	North	Approach	7.670	−4.267	4.459
				Departure	11.849	−4.512	6.562
			South	Approach	6.867	−3.273	4.124
				Departure	6.767	−2.998	3.917
NY	9	Perp_GRS	North	Approach	6.506	−4.049	4.102

State	Test ID	Configuration	Direction	Section	Maximum IRI (m/km)	Minimum RSE (mm)	Maximum RSE (mm)
				Departure	11.325	−7.179	3.309
			South	Approach	9.264	−5.284	4.168
				Departure	5.928	−5.498	3.907
NY	11	Skew_GRS	North	Approach	8.511	−4.615	4.502
				Departure	7.303	−3.455	5.304
			South	Approach	16.881	−4.670	9.860
				Departure	9.715	−2.829	4.684
NY	12	Perp_GRS	N/A	Approach	6.713	−3.162	4.101
				Departure	18.622	−4.980	10.372
NY	101	Perp_Conv	N/A	Approach	26.814	−9.033	14.485
				Departure	47.941	−20.400	12.894
NY	102	Skew_Conv	North	Approach	12.311	−6.059	6.729
				Departure	30.271	−6.183	11.128
			South	Approach	23.840	−11.798	11.025
				Departure	11.106	−2.951	6.659
NY	103	Perp_Conv	N/A	Approach	21.502	−5.637	12.963
				Departure	17.184	−6.162	13.699
NY	104	Perp_Conv	N/A	Approach	14.691	−8.647	8.029
				Departure	8.653	−4.959	4.185
NY	105	Perp_Conv	N/A	Approach	33.355	−10.228	16.235
				Departure	12.473	−6.152	5.975
OH	2	Perp_GRS	N/A	Approach	35.361	−12.080	21.356
				Departure	25.553	−5.447	12.602
OH	3	Perp_GRS	N/A	Approach	37.981	−16.414	17.606
				Departure	42.144	−27.870	24.839
OH	5	Perp_GRS	N/A	Approach	32.608	−12.542	13.516
				Departure	42.598	−25.949	27.034
OH	6	Skew_GRS	East	Approach	12.502	−1.374	3.528
				Departure	16.355	−8.003	4.340
			West	Approach	8.184	−4.352	3.310
				Departure	10.264	−4.954	5.975
OH	7	Perp_GRS	N/A	Approach	11.991	−7.989	5.244
				Departure	7.490	−3.983	6.147

State	Test ID	Configuration	Direction	Section	Maximum IRI (m/km)	Minimum RSE (mm)	Maximum RSE (mm)
OH	8	Perp_GRS	North	Approach	20.051	−11.177	10.902
				Departure	16.695	−6.721	9.473
			South	Approach	13.788	−6.500	7.728
				Departure	20.641	−9.927	14.579
OH	9	Skew_GRS	N/A	Approach	5.892	−4.099	2.652
				Departure	11.890	−6.331	7.395
OH	10	Perp_GRS	North	Approach	19.122	−17.205	10.863
				Departure	33.786	−19.361	11.192
			South	Approach	20.605	−12.336	7.981
				Departure	23.397	−14.888	10.363
OH	11	Skew_GRS	North	Approach	24.090	−15.342	7.377
				Departure	20.790	−10.791	6.786
			South	Approach	30.390	−14.177	11.583
				Departure	15.981	−9.961	3.726
OH	12	Perp_GRS	N/A	Approach	18.455	−4.925	11.147
				Departure	17.941	−4.880	7.727
OH	13	Skew_GRS	East	Approach	12.904	−4.322	6.903
				Departure	11.793	−4.864	4.045
			West	Approach	9.329	−2.918	4.364
				Departure	15.071	−5.440	11.839
OH	14	Skew_GRS	N/A	Approach	16.331	−4.997	8.250
				Departure	14.611	5.875	6.543
OH	15	Skew_GRS	North	Approach	37.684	−22.995	16.562
				Departure	35.358	−15.895	14.930
			South	Approach	28.383	−13.094	18.381
				Departure	38.675	−24.236	15.243
OH	16	Skew_GRS	N/A	Approach	21.121	−6.023	8.459
				Departure	37.777	−24.316	12.108
OH	17	Skew_GRS	N/A	Approach	36.590	−22.801	14.867
				Departure	20.987	−8.121	11.639
OH	19	Skew_GRS	N/A	Approach	10.768	−4.985	7.952
				Departure	12.815	−6.880	4.702
OH	20	Skew_GRS	North	Approach	10.781	−1.772	5.773

State	Test ID	Configuration	Direction	Section	Maximum IRI (m/km)	Minimum RSE (mm)	Maximum RSE (mm)
				Departure	15.732	−4.954	7.209
			South	Approach	9.736	−3.047	4.682
				Departure	8.630	−2.570	6.297
OH	21	Skew_GRS	N/A	Approach	5.037	−0.546	2.493
				Departure	5.843	−2.505	2.921
OH	22	Skew_GRS	East	Approach	6.947	−2.403	4.457
				Departure	7.915	−4.657	1.869
			West	Approach	25.242	−12.632	6.151
				Departure	12.199	−3.049	6.204
OH	23	Perp_GRS	N/A	Approach	21.465	−10.668	5.402
				Departure	62.096	−33.966	23.037
OH	24	Skew_GRS	East	Approach	24.793	−14.805	7.252
				Departure	19.177	−8.249	7.720
			West	Approach	15.785	−10.010	7.615
				Departure	33.911	−17.156	10.652
OH	25	Perp_GRS	North	Approach	13.905	−6.536	8.944
				Departure	10.421	−1.644	3.861
			South	Approach	8.546	−4.887	5.832
				Departure	7.758	−2.687	2.702
OH	26	Perp_GRS	North	Approach	5.621	−2.488	3.251
				Departure	9.799	−2.839	6.623
			South	Approach	7.775	−0.971	3.524
				Departure	8.064	−5.394	5.946
OH	27	Skew_GRS	East	Approach	8.893	−4.915	5.225
				Departure	16.935	−8.185	4.719
			West	Approach	8.237	−2.579	4.486
				Departure	7.191	−2.461	4.512
OH	29	Perp_GRS	North	Approach	9.999	−3.287	5.477
				Departure	9.056	−1.816	5.175
			South	Approach	10.799	−5.272	2.897
				Departure	6.001	−2.942	4.023
OH	30	Skew_GRS	East	Approach	4.597	−2.843	3.856
				Departure	11.882	−3.202	5.766

State	Test ID	Configuration	Direction	Section	Maximum IRI (m/km)	Minimum RSE (mm)	Maximum RSE (mm)
			West	Approach	11.942	−0.730	5.236
				Departure	5.216	−2.541	3.571
OH	103	Perp_Conv	East	Approach	20.976	−10.673	11.375
				Departure	7.079	−1.677	3.646
			West	Approach	7.357	−2.071	2.824
				Departure	18.171	−10.748	11.111
PA	1	Perp_GRS	East	Approach	8.733	−5.042	5.639
				Departure	18.429	−1.868	7.662
			West	Approach	8.775	−1.214	3.142
				Departure	10.212	−3.597	4.586
PA	2	Perp_GRS	North	Approach	33.461	−16.238	11.130
				Departure	23.380	−10.572	10.304
			South	Approach	17.619	−7.226	9.530
				Departure	23.062	−12.400	10.624
PA	3	Skew_GRS	East	Approach	37.057	−14.142	11.292
				Departure	35.535	−15.912	19.958
			West	Approach	14.747	−6.856	8.889
				Departure	37.899	−13.844	15.528
PA	4	Skew_GRS	North	Approach	17.060	−9.606	4.031
				Departure	39.521	−15.098	13.718
			South	Approach	25.574	−11.001	9.260
				Departure	19.282	−10.546	6.542
PA	101	Skew_Conv	North	Approach	14.054	−4.909	6.970
				Departure	22.481	−14.156	8.198
			South	Approach	11.189	−4.199	6.271
				Departure	16.750	−8.073	8.037
SD	101	Skew_Conv	East	Approach	17.392	−11.616	7.551
				Departure	13.933	−4.104	4.564
			West	Approach	15.864	−11.689	6.729
				Departure	10.860	−5.891	3.622
WA	1	Skew_GRS	North	Approach	17.601	−6.834	11.189
				Departure	27.215	−15.580	6.988
			South	Approach	35.692	−20.247	9.932

State	Test ID	Configuration	Direction	Section	Maximum IRI (m/km)	Minimum RSE (mm)	Maximum RSE (mm)
				Departure	17.298	−8.370	7.040
WA	2	Skew_Conv	North	Approach	17.624	−7.697	5.287
				Departure	18.879	−7.307	5.810
			South	Approach	13.565	−7.759	4.863
				Departure	15.546	−8.683	6.119
WI	1	Perp_GRS	North	Approach	32.331	−10.204	14.212
				Departure	19.908	−11.160	15.625
			South	Approach	17.502	−5.077	11.874
				Departure	15.594	−6.187	8.514
WI	101	Perp_Conv	East	Approach	31.351	−17.119	12.244
				Departure	33.050	−22.615	22.183
			West	Approach	22.176	−16.520	15.074
				Departure	38.490	−19.172	19.236
WV	1	Perp_GRS	East	Approach	23.942	−15.909	9.389
				Departure	17.460	−8.305	6.730
			West	Approach	15.314	−10.203	6.835
				Departure	39.336	−16.202	8.230
WV	101	Skew_Conv	North	Approach	20.491	−2.472	10.687
				Departure	10.831	−2.882	5.335
			South	Approach	11.793	−3.045	7.367
				Departure	15.215	−2.658	8.626

1 mm = 0.039 inch; 1 m/km = 5.28 ft/mi.

Table 9. Maximum IRI values and maximum and minimum RSE deviations for Utah bridges.

State	Test ID	Configuration	Direction	Lane	Section	Maximum IRI (m/km)	Minimum RSE (mm)	Maximum RSE (mm)
UT	1	Perp_GRS	N/A	Inside	Approach	5.834	−4.355	3.650
					Departure	11.602	−6.314	2.892
				Outside	Approach	13.301	−5.379	7.132
					Departure	10.569	−6.697	1.403
UT	2	Perp_Conv	East	Inside	Approach	7.686	−4.221	2.714
					Departure	13.196	−7.064	3.972
				Outside	Approach	9.499	−5.847	2.534
					Departure	13.104	−7.812	4.891
			West	Inside	Approach	6.749	−3.862	2.440
					Departure	9.999	−6.673	2.850
				Outside	Approach	6.343	−4.509	2.654
					Departure	9.607	−5.443	2.867

1 mm = 0.039 inch; 1 m/km = 5.28 ft/mi.

REFERENCES

Adams, M., J. Nicks, T. Stabile, J. T. H. Wu, W. Schlatter, and J. Hartmann. 2011. *Geosynthetic Reinforced Soil Integrated Bridge System*, Report No. FHWA-HRT-11-027, Federal Highway Administration, Washington, DC. Available online: https://www.fhwa.dot.gov/publications/research/infrastructure/structures/11027/11027.pdf, last accessed June 5, 2020.

Adams, M., W. Schlatter, and T. Stabile. 2008. "Geosynthetic Reinforced Soil Integrated Bridge System." *Proceedings of EuroGeo4: 4th European Geosynthetics Conference*, paper No. 271, International Geosynthetics Society, Edinburgh, United Kingdom.

AASHTO. 2018. AASHTO R 56-14, *Standard Practice for Certification of Inertial Profiling Systems*, American Association of State Highway and Transportation Officials, Washington, DC.

FHWA. 2004. "23 CFR Part 650—National Bridge Inspection Standards." Federal Highway Administration, Washington, DC. Available online: https://www.govinfo.gov/content/pkg/FR-2004-12-14/pdf/04-27355.pdf, last accessed June 5, 2020.

FHWA. 2019. "Collection Process." (website). Federal Highway Administration, Washington, DC. Available online: https://highways.dot.gov/research/ltpp/data-collection/collection-process, last accessed August 6, 2019.

Henderson, B., J. Dickes, G. Cimini, and C. Olmedo. 2016. *FHWA LTPP Guidelines for Measuring Bridge Approach Transitions Using Inertial Profilers*, Report No. FHWA-HRT-16-072, Federal Highway Administration, Washington, DC. Available online: https://www.fhwa.dot.gov/publications/research/infrastructure/pavements/ltpp/16072/16072.pdf, last accessed June 5, 2020.

Karamihas, S. K. and T. D. Gillespie. 2002. *Development of Cross Correlation for Objective Comparison of Profiles*, Report No. UMTRI-2002-36, University of Michigan Transportation Research Institute, Ann Arbor, MI. Available online: https://deepblue.lib.umich.edu/bitstream/handle/2027.42/1524/97199.0001.001.pdf;sequence=2, last accessed June 5, 2020.

Lee, K. Z. Z. and J. T. H. Wu. 2004. "A Synthesis of Case Histories on GRS Bridge-Supporting Structures with Flexible Facing." *Geotextiles and Geomembranes*, 22 (4), 181–204. Available online: https://doi.org/10.1016/j.geotexmem.2004.03.002, last accessed June 5, 2020.

FHWA. 2019. "LTBP InfoBridge: Data." Available online: https://infobridge.fhwa.dot.gov/data, last accessed June 5, 2020.

McGhee, K. K. 2002. *A New Approach to Measuring the Ride Quality of Highway Bridges*, Report No. VTRC 02-R10. Virginia Transportation Research Council, Charlottesville, VA. Available online: http://www.virginiadot.org/vtrc/main/online_reports/pdf/02-r10.pdf, last accessed May 27, 2019.

Microsoft. 2020. "Bing Maps." Available online: https://bing.com/maps, last accessed November 16, 2020.

Mishra, D., J. McAtee, M. S. Chowdhury, B. C. S. Chittoori, and E. Tutumluer. 2020. *TechNote: Synthesis—The Reduction and Analysis of Pavement Profiler Data to Quantify the Bump at the End of the Bridge*, Report No. FHWA-HRT-20-021, Federal Highway Administration, Washington, DC. Available online: https://www.fhwa.dot.gov/publications/research/infrastructure/structures/bridge/20021/20021.pdf, last accessed June 5, 2020.

Múčka, P. 2016. "International Roughness Index Specifications Around the World." *Road Materials and Pavement Design*, 18 (4), 929–965. Available online: https://doi.org/10.1080/14680629.2016.1197144, last accessed June 5, 2020.

Nicks, J. E. and M. T. Adams. 2018. "Quantifying the Bump at the End of the Bridge with Inertial Profilers Pilot Study: Comparing Deep versus Shallow Foundation Systems." *Presented at the 2018 International Foundations Congress and Equipment Expo*, American Society of Civil Engineers, Reston, VA. Available online: https://doi.org/10.1061/9780784481639.014, last accessed November 12, 2020.

Olmedo, C., B. Henderson, G. Cimini, and J. Springer. 2015. "Bump Determination at Bridge Approach Transitions Using Inertial Profilers." *Presented at the 2015 Conference of the Transportation Association of Canada*, Charlottetown, Prince Edward Island. Available online: http://conf.tac-atc.ca/english/annualconference/tac2015/s18/olmedo.pdf, last accessed June 5, 2020.

Ott, R. L. and M. T. Longnecker. 2015. *An Introduction to Statistical Methods and Data Analysis*, 7th Ed., Cengage Learning, Boston, MA.

Perera, R. W., and Kohn, S. D. 2005. *Quantification of Smooth Index Differences Related to Equipment Type*, Report No. FHWA-HRT-05-055, Federal Highway Administration, Washington, DC. Available online: https://www.fhwa.dot.gov/publications/research/infrastructure/pavements/ltpp/05054/05054.pdf, last accessed December 2, 2020.

Sayers, M. W. and S. M. Karamihas. 1998. *The Little Book of Profiling: Basic Information About Measuring and Interpreting Road Profiles*, University of Michigan Transportation Research Institute, Ann Arbor, MI. Available online: https://deepblue.lib.umich.edu/handle/2027.42/21605, last accessed November 12, 2020.

Schaefer, V. R., A. Maher, J. M. Hooks, and A Foden. 2013. *Summary Report on the FHWA LTBP Workshop to Identify Bridge Substructure Performance Issues: March 4–6, 2010, in Orlando, FL*, Report No. FHWA-HRT-11-037, Federal Highway Administration, Washington, DC. Available online: https://www.fhwa.dot.gov/publications/research/infrastructure/structures/ltbp/11037/index.cfm, last accessed June 5, 2020.

The Transtec Group. 2015. "ProVAL." Available online: http://www.roadprofile.com, last accessed June 5, 2020.

The Transtec Group. 2016. "*ProVAL User's Guide*." Available online: https://www.roadprofile.com/download/ProVAL-3.60-Users-Guide.pdf, last accessed December 23, 2020.

Wang, H. and G. W. Flintsch. 2010. "Comparative Study of Road Profilers' Accuracy and Precision." *Journal of Testing and Evaluation*, 38 (2), 188–94. Available online: https://doi.org/10.1520/JTE101683, last accessed June 5, 2020.

Zang, K., J. Shen, H. Huang, M. Wan, and J. Shi. 2018. "Assessing and Mapping of Road Surface Roughness Based on GPS and Accelerometer Sensors on Bicycle-Mounted Smartphones." *Sensors*, 18 (3), 914. Available online: https://doi.org/10.3390/s18030914, last accessed June 5, 2020.

Recycled
Recyclable

HRDI-40/05-21(WEB)E